Thermal Insulation Foam from Lignin-Phenol-Formaldehyde Resin

Jirapat Romkaew

Ponthep Wongjaikum

Advisor

Asst. Prof. Dr. Natthanon Phaiboonsilpa

A Report Submitted in Partial Fulfillment of the Requirements

for the Degree of Bachelor of Engineering (Petrochemical Engineering)

Department of Chemical Engineering, School of Engineering,

King Mongkut's Institute of Technology Ladkrabang

Academic Year 2022

โฟมฉนวนกันความร้อนจากลิกนินฟีนอลฟอร์มาลดีไฮด์เรซิน

จิรภัทร ร่มแก้ว

พรเทพ วงศ์ใจคำ

ปริญญานิพนธ์นี้เป็นส่วนหนึ่งของการศึกษาตามหลักสูตร

วิศวกรรมศาสตรบัณฑิต สาขาวิชาวิศวกรรมปิโตรเคมี

ภาควิชาวิศวกรรมเคมี คณะวิศวกรรมศาสตร์

สถาบันเทคโนโลยีพระจอมเกล้าเจ้าคุณทหารลาดกระบัง

ปีการศึกษา 2565

Title	Thermal insulation foam from lignin-phenol-formaldehyde resin		
By	Jirapat Romkaew	**Student ID**	62010117
	Ponthep Wongjaikum	**Student ID**	62010590
Field of Study	Petrochemical Engineering		
Advisor	Asst. Prof. Dr. Natthanon Phaiboonsilpa		

Accepted by the School of Engineering, King Mongkut's Institute of Technology Ladkrabang in Partial Fulfillment of the Requirements for the Degree of Bachelor of Engineering (Petrochemical Engineering).

Thesis Committee

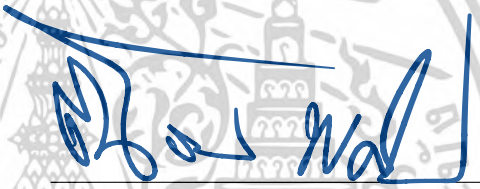

_____ Chairman
(Asst. Prof. Dr. Natthanon Phaiboonsilpa)

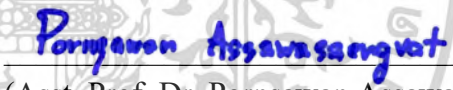

_____ Committee
(Asst. Prof. Dr. Pornsawan Assawasaengrat)

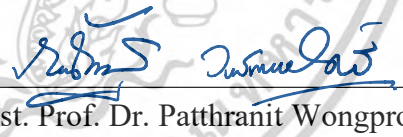

_____ Committee
(Asst. Prof. Dr. Patthranit Wongpromrat)

Title	Thermal insulation foam from lignin-phenol-formaldehyde resin		
By	Jirapat Romkaew	**Student ID**	62010117
	Ponthep Wongjaikum	**Student ID**	62010590
Advisor	Asst. Prof. Dr. Natthanon Phaiboonsilpa		
Field of Study	Petrochemical Engineering		
Affiliation	Department of Chemical Engineering, School of Engineering King Mongkut's Institute of Technology Ladkrabang		

Abstract

Sugarcane has been one of the main agricultural products of Thailand with production of 106 Mton per year in 2021. Sugarcane bagasse is a leftover from sugar production of sugarcane. In sugarcane bagasse compose of lignin 30% by weight. Lignin is a large structure polymer composes of monomers or small units of lignin, which has similar structure to phenol. Replacing phenol with lignin would help in solving resources shortage in the future using renewable sources. Phenol-formaldehyde resin or phenolic resin has been manufactured and used around the globe; thermal insulation foam is one of the phenolic resin applications. Physical property, morphology, and thermal conductivity were studied after had replaced phenol with lignin for phenolic foam in this research. Phenolic resin was synthesized and foaming with same formular. Results exhibited good trend when replacing phenol with lignin. Pore diameter and density of foam increased with lignin replacement. However, thermal conductivity decreased with presence of lignin, but percentage of lignin do not affect much. The results supported possibility of replacing phenol with lignin in thermal insulation foam from phenolic resin though some further investigation must be conducted.

Keywords: Foam, Insulation, Lignin, Delignification, Phenol-formaldehyde resin, Sugarcane bagasse, Phenol substitution

เรื่อง โฟมฉนวนกันความร้อนจากลิกนินฟีนอลฟอร์มาลดีไฮด์เรซิน
โดย จิรภัทร ร่มแก้ว **รหัสนักศึกษา** 62010117
พรเทพ วงศ์ใจคำ **รหัสนักศึกษา** 62010590
อาจารย์ที่ปรึกษา ผู้ช่วยศาสตราจารย์ ดร. ณัฐนนท์ ไพบูลศิลป์
สาขาวิชา วิศวกรรมปิโตรเคมี
สังกัด ภาควิชาวิศวกรรมเคมี คณะวิศวกรรมศาสตร์
สถาบันเทคโนโลยีพระจอมเกล้าเจ้าคุณทหารลาดกระบัง

บทคัดย่อ

อ้อยเป็นหนึ่งในผลผลิตทางการเกษตรหลักของประเทศไทย โดยมีปริมาณการผลิตถึง 106 ล้านตันต่อปีอ้างอิงจากปี ค.ศ. 2021 ชานอ้อยเป็นหนึ่งในของเหลือที่ได้จากการผลิตน้ำตาลของอ้อย ในชานอ้อยมีลิกนินเป็นส่วนประกอบถึงร้อยละ 30 โดยมวล ลิกนินเป็นพอลิเมอร์ที่มีโครงสร้างขนาดใหญ่โดยประกอบขึ้นจากมอนอเมอร์หรือหน่วยย่อยขนาดเล็กโดยหน่วยย่อยของลิกนินมีโครงสร้างคล้ายคลึงกับฟีนอล การนำลิกนินมาแทนที่การใช้ฟีนอลจะช่วยในการแก้ปัญหาการขาดแคลนของทรัพยากรในอนาคตโดยใช้ทรัพยากรหมุนเวียนได้ ฟีนอลฟอร์มาลดีไฮด์เรซินหรือฟีนอลิกเรซินเป็นเรซินที่มีการผลิตและใช้งานทั่วโลก หนึ่งในการใช้งานของฟีนอลิกเรซินคือการนำไปทำเป็นโฟมฉนวนกันความร้อน คุณสมบัติเชิงกายภาพ สัณฐานวิทยาและการนำความร้อนของโฟมจะถูกศึกษาหลังมีการแทนที่ฟีนอลด้วยลิกนินในงานวิจัยนี้ เรซินจะถูกสังเคราะห์ขึ้นและนำไปขึ้นรูปโฟมโดยใช้อัตราส่วนที่มีการศึกษาก่อนหน้า ผลลัพธ์ที่ได้แสดงให้เห็นถึงแนวโน้มที่ดีขึ้นเมื่อแทนที่ฟีนอลด้วยลิกนิน ขนาดเส้นผ่านศูนย์กลางรูพรุนและความหนาแน่นของโฟมเพิ่มขึ้นเมื่อแทนที่ฟีนอลด้วยลิกนิน นอกจากนี้หลังจากมีการแทนที่ของลิกนินแล้วการลดลงอย่างเห็นได้ชัดของค่าการนำความร้อนโดยที่จำนวนที่ใส่เพิ่มไม่ส่งผลมากนัก ผลลัพธ์ที่ได้สนับสนุนความเป็นไปได้ของการแทนที่ลิกนินในฉนวนกันความร้อนฟีนอลิกโฟมแต่จำเป็นที่จะต้องมีการศึกษาเพิ่มเติมในบางส่วน

คำสำคัญ: โฟม ฉนวนกันความร้อน ลิกนิน การแยกลิกนิน ฟีนอลฟอร์มาลดีไฮด์เรซิน ชานอ้อย การแทนที่ฟีนอล

Acknowledgement

With the deepest gratitude, the author wishes to express sincere gratefulness to Asst. Prof. Dr. Natthanon Phaiboonsilpa, Department of Chemical Engineering, School of Engineering, King Mongkut's Institute of Technology Ladkrabang, for his fruitful guidance and perpetual supervision throughout this research. His willingness to give his time so generously has been very much appreciated. The author also would like to express thankfulness to Asst. Prof. Dr. Surat Areerat for his valuable discussions, time, and great assistance with experimental guidelines and analysis of experimental results on this research. We would like to thanks to Department of Chemical Engineering, King Mongkut's Institute of Technology Ladkrabang, Advanced Manufacturing Innovation Central Lab, The Joint Graduate School of Energy and Environment, technician scientists, and technicians of the laboratory for giving us advice and assistance for resources in this research. Finally, we most gratefully acknowledge my parents, my family, and my Department of Petrochemical Engineering friends for suggestions, advice, moral support, and all their help throughout the period of this research.

Jirapat Romkaew

Ponthep Wongjaikum

Table of Contents

List of Figures

List of Tables

Nomenclature

Abbreviation Title	Full Title
PF	Phenol-formaldehyde
LPF	Lignin-phenol-formaldehyde
ASEAN	Associate of Southeast Asian Nation
BaO	Barium oxide
MgO	Magnesium oxide
CaO	Calcium oxide
ZnO	Zinc oxide
H_2CO_3	Carbonic acid
F/P	Formaldehyde to phenol ratio
AG	Analysis grade
SEM	Scanning Electron Microscope
BET	Brunauer-Emmett-Teller
N_F	Cell density
n	number of cells
A	Cross-sectional area
k	Thermal conductivity
q	Heat flux
∇T	Temperature gradient
T	Temperature
τ	Time
ρ	Density
C_p	Thermal capacity per volume of material
EPFA	European Phenolic Foam Association
NaOH	Sodium hydroxide
KOH	Potassium hydroxide
$Ba(OH)_2$	Barium hydroxide

Abbreviation Title	Full Title
$Ca(OH)_2$	Calcium hydroxide
GC	Gas chromatography
MS	Mass spectrometry
GPC	Gel permeation chromatography
Mw	Weight-average molecular weight
BPF	Bio-based phenol formaldehyde
PTFE	Polytetrafluoroethylene
rpm	Revolutions per minute
W_1	Weight of cured sample before reflux
W_2	Weight of cured sample after reflux
ASTM	American Society for Testing and Materials
Q	Amount of heat flowing through sample
L	Distance between measuring temperature
Q_{Actual}	Applied heating power at heat source side
Q_{loss}	Heat losses from convection and radiation
KLPF	Kraft lignin-phenol-formaldehyde
1-LPF-10%	phenol-formaldehyde with 10% 1^{st}-stage lignin
1-LPF-50%	phenol-formaldehyde with 50% 1^{st}-stage lignin
KLPF-10%	phenol-formaldehyde with 10% kraft lignin
KLPF-50%	phenol-formaldehyde with 50% kraft lignin
2-LPF-10%	phenol-formaldehyde with 10% 2^{nd}-stage lignin
2-LPF-50%	phenol-formaldehyde with 50% 2^{nd}-stage lignin

CHAPTER 1
INTRODUCTION

1.1 Backgrounds of the research and its significance

Phenol-Formaldehyde (PF) resin, also known as phenolic resin, are widely used in many applications such as adhesives, carbon foams, molding compounds, and fire-resistant composites (Yang, et al., 2020). Its wide range of application is due to its excellent heat and flame retardancy, high mechanical strength, great electrical and thermal insulation, and good chemical resistance (Takeichi & Furukawa, 2012).

Phenolic resin is prepared by condensation polymerization between phenol and formaldehyde using acid or alkali as a catalyst. The reaction can result in two types; resole resin and novolac resin (Daothong & Yingsirisit, 2021). The resulting resin can be chosen by varying molar ratio of formaldehyde to phenol. However, phenols used in phenolic resin are from petroleum sources which is now facing shortage of petroleum. Hence, finding substitution for phenol in synthesizing phenolic resin is crucial.

Phenolic foams' properties allow them to be applied in some specific applications, such as wastewater treatment or insulation building material. The global market of insulation foam is in billion euros (Mougel, Garnier, Cassagnau, & Sintes-Zydowicz, 2019). Phenolic foams are well known as rigid thermosetting foams with good thermal insulation, high thermal stability, highly retard to flame and low amount of toxic gases as a result of combustion (Li, Wang, & Tsai, 2016).

Sugarcane is one of the key economic agricultural products in Thailand. Total production of sugarcane in 2020/2021 is about 106 Mt (Office of the Cane and Sugar Board, 2021). The sugarcane itself mainly used to produce sugar while sugarcane bagasse and molasses, the waste from the production, are used in producing electricity and ethanol respectively (Prasara-A, Gweewala, Silalertruksa, Pongpat, & Sawaengsak, 2019). The sugarcane bagasse is like any other biomass, it composes of 3 components, cellulose, hemicellulose, and lignin as 40%, 30%, and 30% by weight respectively. The bagasse waste from sugar industry is a potential candidate as a renewable source of chemicals, replacing petroleum-based one.

Lignin is the second highest mass founded in natural polymer after cellulose and has second most effect on mechanical strength and stiffness on plants (Pfungen, 2015) . Structures of lignin are complex due highly branched phenylpropanoid network, consist of three abundant repeating units; methoxylated coumaryl, coniferyl, and sinapyl alcohols (Grishechko, et al., 2018) . Lignin has been investigated by numerous researchers for various applications. It is left as a waste from sugarcane bagasse. Many of previous studies have proved that lignin can crosslink with phenol and formaldehyde in production of phenolic resin resulted as lignin-phenol-formaldehyde resin.

To determine the feasibility of replacing phenol with lignin from sugarcane bagasse in lignin-phenol-formaldehyde foam as thermal insulation material. Thermal properties of foams must be examined and compared with the result of commercial phenolic foam. In previous studies, suitable conditions and methods of lignin extraction have been founded and will be used in our studies.

1.2 Objectives

1.2.1 To synthesize insulation foam from lignin-phenol-formaldehyde (LPF) resin using liquefied lignin obtained from sugarcane bagasse.

1.2.2 To study morphology and thermal conductivity of LPF foam.

1.3 Scopes of work

1.3.1 Amount of formaldehyde and sodium hydroxide remain same in all formulation.

1.3.2 Find optimal reaction time of PF resin and used it throughout all formulation.

1.3.3 Substitute phenol with kraft, 1st-stage and 2nd-stage lignin for 10 wt.% and 50 wt.%.

1.3.4 Study morphology and find thermal conductivity of PF and LPF foam

1.4 Expected outputs

1.4.1 LPF resin's thermal conductivity should be better than PF resin.

1.4.2 2nd-stage lignin should have similar morphology and thermal conductivity as PF foam due to presence of phenolic monomers.

1.4.3 1st-stage lignin should have better results than commercial kraft lignin due to difference in isolation method.

CHAPTER 2
THEORY AND LITERATURE REVIEWS

This chapter refers to the components of biomass and the most important part of biomass which is lignocellulose. Details of each component in lignocellulose such as cellulose, hemicellulose, and lignin as well as basic theory of phenol formaldehyde resin include of gel drying methods and related literature reviews will be described in this section.

2.1 Biomass composition and structure

Biomass is an organic compound that refers to the mass of living organisms of both plants and animals. The most common biomass material feedstocks are plants, wood, and waste. Biomass material feedstocks have been considered one of alternative ways substituting petroleum-based resources. The energy from biomass can be converted into usable energy, electricity, or biofuel by thermal and chemical conversion. Generally, Biomass consists of three main constituents:

1. Moisture is the water component existing in biomass mostly found in biomass from agricultural.
2. Combustible substances are hydrocarbons consisting of carbon, hydrogen, and oxygen atoms. They can be classified into two types, volatile matter, and fixed carbon.
3. Ash or non-combustible substance is an inorganic compound with no ability converting to usable energy.

Thailand is the largest producer of sugarcane and sugar in ASEAN as well as the world's second-largest exporter (Bio-Industry Promotion Group Division of Cane Industry, 2560). Bagasse is a by-product of sugar manufacturing. The added value for bagasse as the biomass is considered in this work. The heterogeneous fibrous residue remains, after sugarcane stalks are crushed for sugar production. When the heterogeneous fibrous residue is dried, bagasse comprises of 45% cellulose, 28% hemicellulose, 20% lignin, 5% sugar, 1% minerals, and 2% ash.

2.1.1 Lignocellulose

Lignocellulose is abundant in bio-renewable material on earth which consists of three main components such as cellulose, hemicelluloses, and lignin. It is mostly found in cell wall of plant cell in both monocotyledon and dicotyledon. On average, lignocellulose consists of 20-30% hemicellulose by mass, 40-50% cellulose by mass, and 20-30% lignin by mass. (Nunes & Kunamneni, 2018)

2.1.2 Cellulose

Cellulose is an organic compound found in plant cell as the polysaccharides by the chain of homopolysaccharide made up of D-anhydro-glucopyranose linked by β-1,4-glycosidic linkages with the formular of $(C_6H_{10}O_5)_n$

where n represents the repeating units with range of 10-10,000 units. Structure of the polymer is straight chain that composes of repeating units of cellulose called cellobiose. Each of straight chain called fibril which links with intermolecular force of hydrogen bonds between the hydroxyl groups causes the appearance of crystallinity. Destruction of the polymer structure of cellulose is difficult because the crystal structure is strong and disordered. However, some structures of cellulose are disordered, resulting in a semi-crystalline structure. This semicrystalline structure is called semicrystalline cellulose. (para-crystalline cellulose) where the polymer structure can be destroyed easier than the crystalline structure. Cellulose has resistant to strong alkali solvent (17.5 wt.%) and oxidizing agents but easily hydrolyzed to smaller molecules by acid to water-soluble sugar

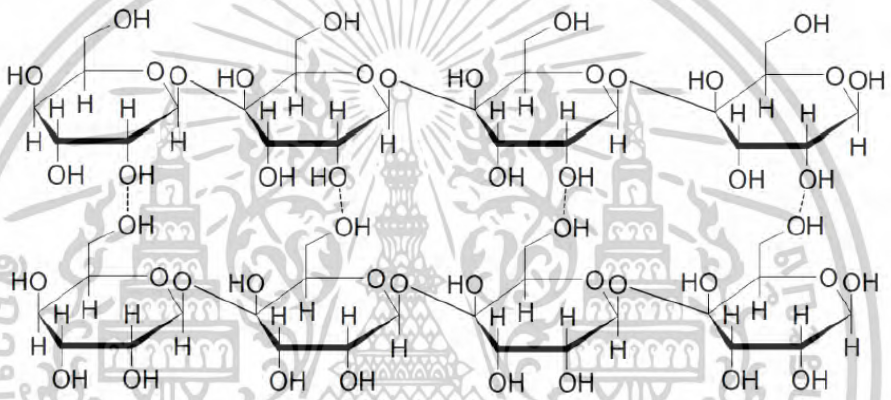

Figure 2.1 Cellulose structure with hydrogen bonds represent in cellulose molecule, represented by dashes (---) (V.Karpe, 2015).

2.1.3 Hemicellulose

Hemicelluloses are branched chain polymers as shown in Figure 2.2 and they have a higher molecular weight than cellulose. It consists of five-carbon monosaccharides (xylose and arabinose) and six-carbon monosaccharides (glucose, galactose, and mannose) joining chain together and have alkyl group connected as branched chains results in the formation of amorphous structure for hemicellulose. It is easier to break the polymer chain of hemicellulose than cellulose that consists of crystalline structure. The linkage between five-carbon monosaccharides (xylose and arabinose) and six-carbon monosaccharides (glucose, galactose, and mannose) is mostly accomplished through β-(1,4) glycosidic linkages.

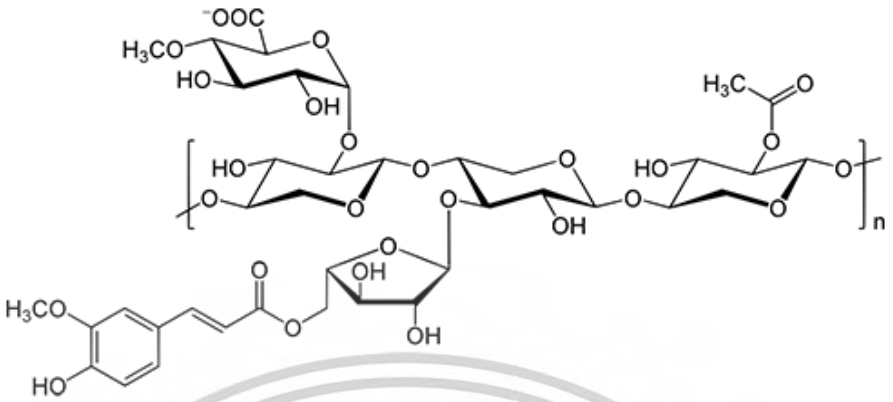

Figure 2.2 Example of polymers in hemicellulose (xylan).

Moreover, hemicellulose is closely linked with lignin via acid ester linkage as lignin-carbohydrate complex and with cellulose via extensive hydrogen bonding. When hemicellulose combined with cellulose and lignin, Hemicellulose may help plant cell walls to be strong and flexible. due to its hydrophilic nature It also helps to retain water in the cell walls of plants. (B. Kamm, M. Gerhardt, G. Dautzenberg, 2013)

2.1.4 Lignin

Lignin is a plant-derived amorphous hetero-biopolymer. The main components for plants and wood which formed by three phenolic compounds as monolignols or phenyl propane unit. The name of lignin is different based on the how that lignin obtained from. Derivatives of lignin can be represented in Figure 2.3 which are p-coumaryl alcohol, coniferyl alcohol, and sinapyl alcohol. All of these are built up with a phenolic hydroxyl group, methoxy groups, and propyl side chain with different number of methoxy group (OMe).

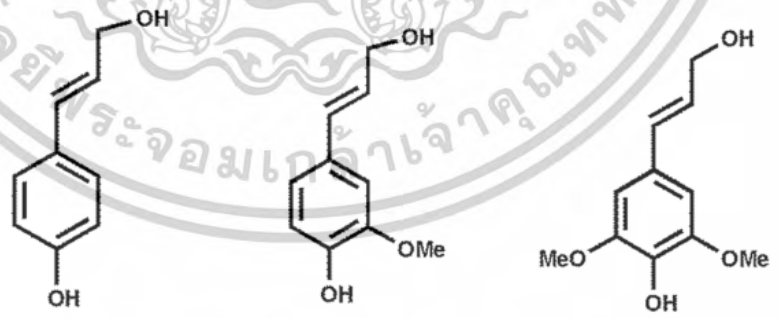

Figure 2.3 The building blocks of lignin consist of three primary types of monolignols, namely p-coumaryl alcohol (left), coniferyl alcohol (middle), and sinapyl alcohol (right). (Caihong, Xiaowei, & Yejun, 2021)

Structure of macromolecule of lignin composes of three phenylpropanoid units linked with the chemical bonds of aryl ether (β-O-4'), phenylcoumaran (β-5'), resinol (β-β'), biphenyl ether (4-O-5'), and dibenzodioxocin (5–5') as illustrated in Figure 2.4

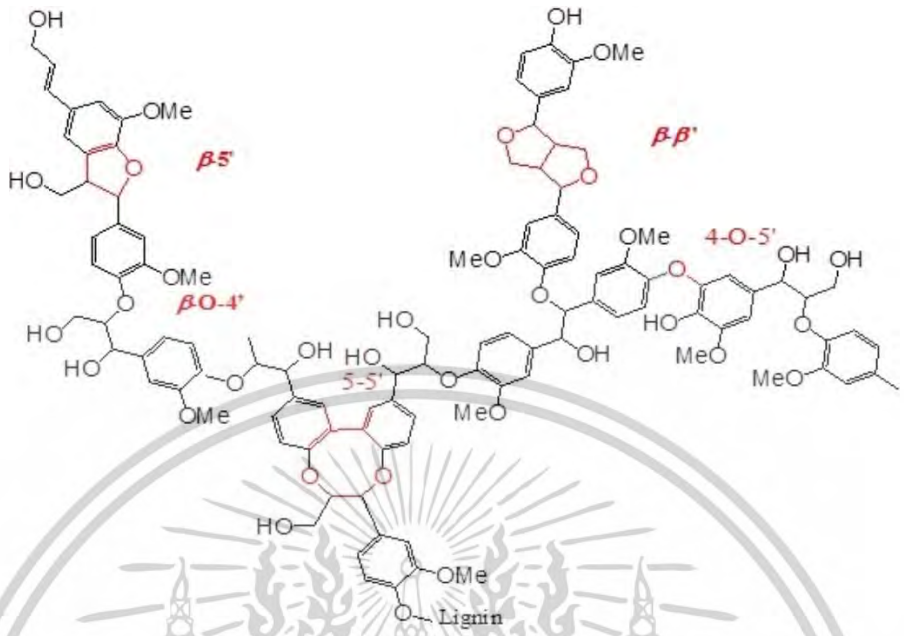

Figure 2.4 Structure macromolecule of lignin consists of different chemical bonds linkage (e.g., β-O-4, β-β, 5–5, and β-5) (Naseem, et al., 2016).

2.2 Methods of lignin isolation

Cellulose, hemicellulose, and lignin are the main components of lignocellulose as mentioned before. The method of lignin extraction is used to isolate lignin out of other components or delignification process. There are several ways to extract lignin. Typically, the popular approach is chemical processes such as kraft pulping process, Klason lignin method, and Organosolv method.

2.2.1 Delignification by kraft pulping process

kraft lignin is a kind of industrial lignin obtained from kraft pulping or soda pulping process under alkaline condition by using sodium hydroxide and sodium sulfide to dissolve lignin. The extracted lignin is obtained in the form of black liquor and the solid residue contains cellulose with other components of lignocellulose. Chemical reaction takes an action to Na^+ connecting with phenolic hydroxyl groups (-OH) and carboxyl acid groups (-COOH) of lignin then forming the phenolic sodium (-CONa) and carboxylate sodium (-COONa) group. (Guo, Wu, Liu, Yin, & Yang, 2012) as alkali lignin that is soluble in water. Thus, sodium salts in black liquor are represented in two forms as NaOH and Na_2CO_3 as ionic species associated with water.

2.2.2 Delignification by Klason lignin method

Isolated lignin from this method is obtained through hot water or strong acid such as sulfuric acid (H_2SO_4) and hydrochloric acid (HCl) to promote carbohydrate hydrolysis then it is diluted with water, filtered, washed, and dried. Therefore, solid residue refers to lignin. (G. Calvo-Flores, A. Dobado, Isac-Garcia, & J. Martin-Martinez, 2015)

2.2.3 Delignification by Organosolv method

Sulfur-free chemical is used for delignification in this process. The most commonly used solvents are ethanol, methanol, acetic and formic acids. The isolation method of lignin with these solvents usually performs at temperatures of 170–190°C. The use of high-boiling solvents makes it possible to carry out the better delignification result at atmospheric pressure. As a result, lignin-carbohydrate bonds are mainly destroyed, whereas β-O-4' bonds are less prone to cleavage causes structure of lignin can be keep and preserved without any destruction from the solvents. Moreover, this process tends to be more environmentally friendly because it does not require sulfur-containing compounds or severe conditions and keep the value of lignin. (O. V. Arapova, A. V. Chistyakov, M. V. Tsodikov, I. I. Moiseev , 2020)

2.3 Lignin conversion to phenolic monomers

(Anantkijthamrong, 2016) study one-step and two-step conversion of lignin to phenolic monomers. As preliminary comparation, one-step conversion method found the undissolved metal catalyst were found to contaminate in the cellulose-rich residue, which caused serious drawback in further use of residual catalyst. So, the two-stepwise conversion of lignin to phenolic monomers was proposed. Hemicellulose and lignin in plant cell wall were hydrothermal liquefied under alkaline condition without metal catalysts in the first stage. Liquefied portion from first stage were subjected to oxidative depolymerization by using hydrogen peroxide with copper (II) oxide and iron (III) sulfated catalyst. The study found that relatively pure cellulose content in residue of extractives-free sugarcane bagasse was obtained in the first stage hydrothermal liquefaction, while the liquefied portion could end up with monophenolic aldehydes in the second stage oxidative depolymerization in the presence of metal.

(Srichan, 2020) explored the optimization of two-step lignin depolymerization from sugarcane bagasse to phenolic monomers compounds under alkaline conditions using hydrogen peroxide with copper (II) oxide and iron (III) sulfated catalyst. The report shown the highest yield of phenolic monomers, about 11.2wt% produced by using liquefied lignin obtained by 4%w/v 140ºC in the first stage and treated at 190ºC in the second stage. At the optimum point, the composition of phenolic monomers compound composed of hydroxybenzaldehyde and hydroxybenzoic, namelt p-type lignin, were found as the major products.

2.4 Phenol formaldehyde resin

2.4.1 Phenol-formaldehyde resin

Dr. Baekeland invented phenol-formaldehyde resins in 1909. The patent has laid the industrialization foundation of phenol-formaldehyde resins (phenolic resins). Phenolic resin is a condensate polymer synthesized by condensation polymerization between phenols, such as phenol, cresol, and resorcinol, and aldehydes, such as formaldehyde, acetaldehyde, and furfural, at a set temperature with acid or alkali catalyst. Phenolic resin is widely used in many fields e.g., electronic,

construction, aerospace, and machinery due to its availability and low cost of raw materials, simple processes and equipment, great mechanical properties, heat and chemical resistance, electrical insulation, and flame retardance.

The hydroxyl groups in phenol and methylene groups in molecule of phenolic resin are easily oxidized. Critical thermal decomposition occurs when the temperature exceeds 250 ºC affecting its heat and oxidation resistance. The benzene ring in the molecule's structure of phenolic resin is connected by a methylene group only, this causes the density of the benzene group (rigid group) to be large. The packing is tight, the steric hindrance is large, and the degree of freedom of the link rotation is small, resulting in poor toughness.

The molecular structure of phenolic resin can be impacted by factors, the molar ratio of monomer, the number of functional groups of the monomer and the type of catalyst. There are three types of catalysts that are commonly used in the preparation of phenolic resin, which are alkaline catalysts, alkaline earth metal oxide catalysts, and acid catalysts. The most used alkaline catalysts are sodium hydroxide, 25% (mass fraction) ammonia water, and barium hydroxide. For alkaline earth metal oxide catalysts that are commonly used include BaO, MgO, CaO, and ZnO. The effect of the earth metal oxide catalysts is weaker than that of alkaline catalysts, but it can be used to prepare high-ortho phenol resin. Acid catalysts that are commonly used include hydrochloric acid, H_2CO_3 and organic acids (Tang, et al., 2020).

The mechanism between phenol and formaldehyde is known to be initiated by the activation of benzene ring by the hydroxyl group joining the benzene at ortho- and para-positions. The reaction results in a resole if an alkaline catalyst is used and a novolac for an acid catalyst (Pizzi & Ibeh, 2014).

2.4.1.1 Resole resin

Resole phenol-formaldehyde resins are produced by condensation polymerization with molar ratio of formaldehyde to phenol of 1 or more with the presence of an alkaline catalyst at 80-100 ºC for 1 hour. The common molar ratio is 1.1 to 1.5. The resole resin is a water-soluble thermoplastic with methylol. The curing process to the finalized thermoset material can be started by heating resole in a mold. After heated, resole molecules are larger due to methylene cross-links. Water is given off as a by-product.

Resole reaction can be categorized into three stages:

1. A-stage or resole.
2. B-stage or resitol.
3. C-stage or resite.

The products in the A-stage are mainly alcohols on benzene ring. The resin during this stage is thermoplastic and can be dissolve in inorganic solvents. At the B-stage, the degree of condensation and cross-linking between resin is higher with an increase in molecular weight and viscosity, and a decrease in solubility. During

this stage, the resin is soft and fusible when heat, but hard and brittle when cool down. At the C-stage, the degree of polymerization and cross-linking is very high and nearly completed. The resin in this stage is insoluble and infusible (Pizzi & Ibeh, 2014).

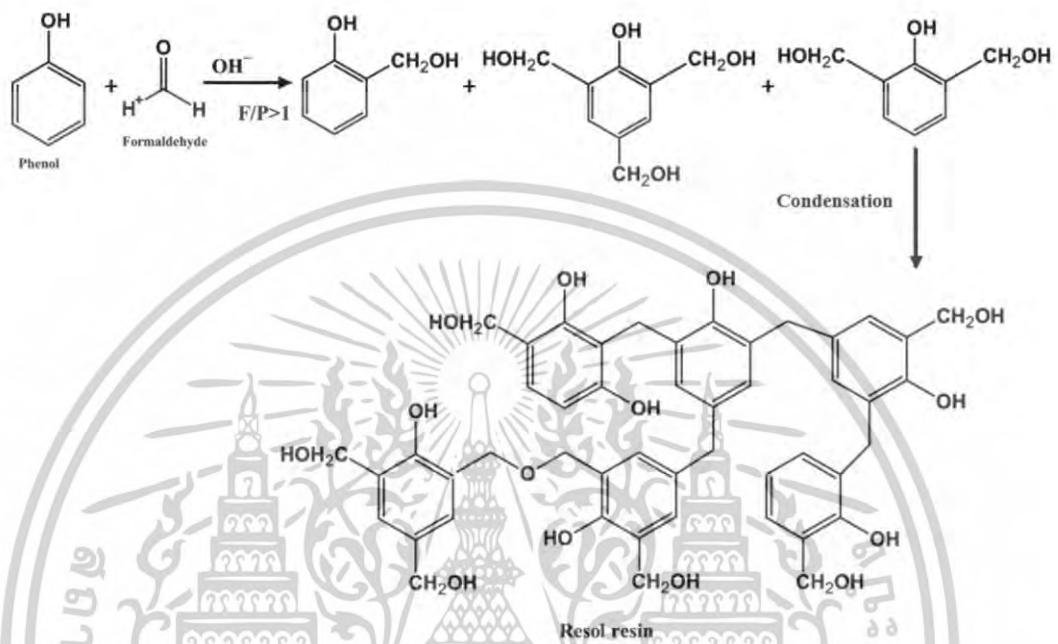

Figure 2.5 Resole resin synthesis (Sarika, Nancarrow, Khansaheb, & Ibrahim, 2020).

2.4.1.2 Novolac resin

The polymerization of phenolic novolac resin is performed with the presence of an acid catalyst, sulfuric and oxalic acids are the two most used. The formaldehyde to phenol molar ratio is 0.8 in the pre-polymerization stage. The reaction is carried out by heating the mixture for 2 to 4 hours with water removal at 160°C. The glassy resultant is then crushed and blended with curing agent to produce a molding compound. The compound is then heated to 165°C in a mold to provide the final curing.

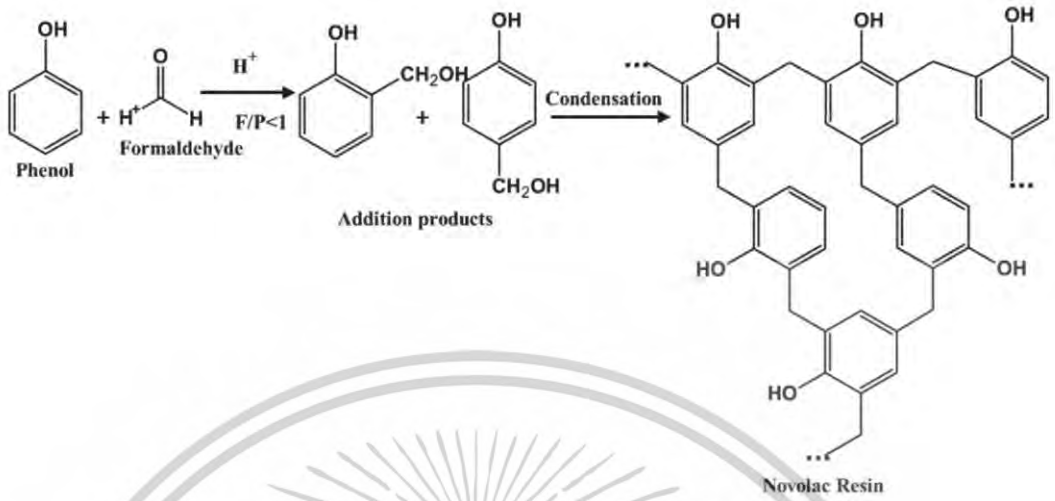

Figure 2.6 Novolac resin synthesis (Sarika, Nancarrow, Khansaheb, & Ibrahim, 2020).

2.5 Phenolic foams

Plastic foams or polymeric foams, phenolic foam included, generally have a minimum of two phases, a solid polymer and a gaseous phase created by a blowing agent. This phase can be organic, inorganic, or organometallic. Solid phase can be composed by polymer alloys or polymer blends based on twos or more polymer. Other possible solid phases present in the foam are fillers, either fibrous or other-shaped fillers. The foams' mechanical properties depend on many factors, their chemical composition, degree of crystallinity, and degree of crosslinking. For the factors that affect other properties, size, shape, and cell geometry of the foams are the causes. The produced foams densities range from 1.6 kg/m^3 to over 960 kg/m^3 (Landrock, 1995).

Among foams that has been commercialized, phenolic foams are known as rigid thermosetting foams with good thermal insulation, excellent fire retardance, stable in high temperature condition, no wetting behavior and low toxic gases occurred during combustion (Li, Wang, & Tsai, 2016). The brittleness of phenolic resin is restricting its foam application (Landrock, 1995) , so it is crucial to improve the mechanical properties of phenolic foam while not alter its thermal properties. The improvement can be done via two routes, foam formulation and the production process. The first route is the changes of component and its amount used in foam formation to optimize the foam properties for desired application (Gardziella, Pilato, & Knop, 2000). The second route is the selection of the production process. Using an open mold result in higher content of open cells and inhomogeneous density, while closed mold results in more controllable density and higher content of closed cells.

2.5.1 Principles of foam formation

The formation of a polymeric foams starts with the formation of gas bubbles in a liquid phase of polymer (Bubble Nucleation), then the bubble will grow

bigger (Bubble Growth) and stabilize as the viscosity of the liquid polymer increases until the polymer become solidified as cellular resin matrix (Landrock, 1995).

Foam manufacturing can be done by two fundamental methods, dispersing a gas into continuous liquid phase creating colloidal system and generating gas in liquid phase and appears as dispersing bubbles in liquid phase (Landrock, 1995). There are many commonly used foaming methods such as thermal decomposition of a blowing agent, volatilization of gaseous products from exothermic reaction, volatilization of a low-boiling point solvent, mechanical agitation of gaseous products, expansion of a dissolved gas by reducing system pressure (Landrock, 1995). For phenolic foam production, the commonly used methods consist of volatilizing of low-boiling point solvent, or gases produced during exothermic polymerization reaction, and thermal decomposition of chemical blowing agents by heating (Pilato, 2010).

The compositions used in phenolic foam formation are the phenolic resin itself, emulsifier, blowing agent, catalyst, and additives as optional properties modification.

Emulsifiers are of great importance because they help in controlling foam quality and properties. They are used for generating a stable and homogenous emulsion between the blowing agent and the resin that affect the foam cell characteristics. The main challenge of emulsifier is to assure the stability of emulsion during entire foaming process, including increasing of temperature, viscosity and state changes of blowing agent (Pilato, 2010). Polyethylene glycol sorbitan monooleate or Tween 80 is a non-ionic surfactant that is mostly used in foam formation (Yuan, Zhang, & Wang, 2015). Silicon oil can also be used as an alternative for Tween 80 (Yuan, et al., 2012). The non-ionic surfactant generally helps in the opening of the cells. An anionic surfactant helps to break the resin encapsulating blowing agent, which also acts as demulsifier that helps creating interconnected open cell pore structure of foam by vaporizes blowing agent during bubble collision and combination (Xu, Gong, Cui, Liu, & Li, 2014).

Blowing agents are known to be responsible for creating bubbles in foaming process via physical or chemical processes. Blowing agents which are used in physical process are generally low boiling point liquids thus generating gas bubble in polymer matrix as temperature increases from external heating and/or exothermic reaction between resin and acid catalyst. These blowing agents are the most commonly used (Mougel, Garnier, Cassagnau, & Sintes-Zydowicz, 2019). Other type of blowing agents is generating gas bubble via chemical reaction, some are reaction of carbonates with acid catalyst (Pilato, 2010) or reaction of water with isocyanate in small amount.

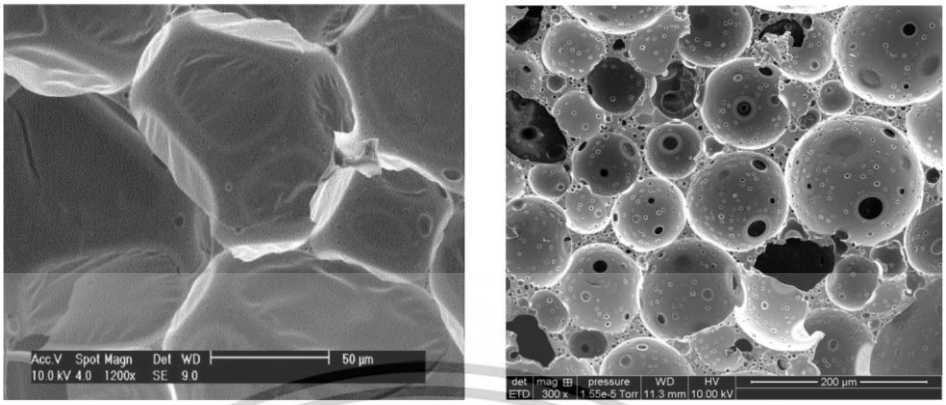

Figure 2.7 Closed cell (Left) and open cell phenolic foam (Right) (Mougel, Garnier, Cassagnau, & Sintes-Zydowicz, 2019).

Type of blowing agents affect the foam cell structure, creating foams with either open or closed cell (Figure 2.7). Choosing the type of blowing agent depends on the final (Nasir, et al., 2011)application and desired cell type. To produce open cell foam that is used as adsorbent, high volatile hydrocarbons are used because of their low boiling point and to limit the risk of explosion. Pentane is used the most in phenolic foam manufacturing (Li, Wang, & Tsai, 2016). For closed cell foam has been widely used for building insulation applications, the used blowing agent trapped inside the cells. This affects overall thermal conductivity of phenolic foam which directly influence the insulation properties of the foam (Pilato, 2010). Chlorofluorinated blowing agents were widely used but due to its damage to environment, they have to be blend with pentane or isomers that have no environmental impact (Mougel, Garnier, Cassagnau, & Sintes-Zydowicz, 2019).

Catalysts are required for resole based phenolic foam to reduce gelation time for accelerating curing reaction of resin. At the present, organic acids, such as p-toluene sulfonic acid (Li, et al., 2016), are commonly used. They are preferred to corrosive inorganic acid, such as sulfuric acid (Pilato, 2010). Blending organic acid with small portion of inorganic acid to increase reaction rate.

The curing of phenolic foam can be done under acidic and/or thermal conditions, to accelerate the curing reaction both conditions are used (Landrock, 1995). At the same time as curing reaction occurs, the blowing agent volatilization expands foam mixture. Foam formation must be completed before the resin is completely crosslinked.

The formation of foam can be controlled by the competition between two mechanisms, the expansion of blowing agent and the curing of resin that occurs simultaneously. Two key parameters are the viscosity and the reactivity of phenolic resin. The viscosity of phenolic resin has been reported to influence structural characteristics such as the cell wall thickness and size of the cells (Pilato, 2010). Too high viscosity can restrict the foam expansion and lead to higher density. For the resin

reactivity, it controls the curing and foaming processes (Gardziella, Pilato, & Knop, 2000) . Too high reactivity will cause the foams to be cured before foaming is completed and final density will differ. Other parameters that also have effects on final foam properties are pH, water content, and amount of monomers (Mougel, Garnier, Cassagnau, & Sintes-Zydowicz, 2019).

2.5.2 Foaming production processes

Phenolic foam has been industrially produced via many processes, batch, continuous or semi continuous processes (Pilato, 2010) . There is also an unconventional process that was developed recently, microwave foaming, but it has not been industrialized into scaled up process yet.

The batch process is the easiest and uses least start-up cost despite high operating cost (Pilato, 2010). The resin and emulsifiers are mixed together with other additives in a container using rotating paddle stirrer. Then the solution is mixed with blowing agent and acid catalyst, resulting in foaming mixture which then is poured into a mold varying form and size depending on application. The foaming process is supplied heat by external heating at 50 - 80 °C to expand and cure the resin (Pilato, 2010). The mold can be open or closed, depending on final product design. Once the curing is completed, the foam blocks are demolded, dried and post curing is perform depending on application.

The continuous process is more expensive to implement but uses less operation cost and results in higher quality and reproducibility of foam. The most important parameters are the mixing head and its characteristics. The process starts with feeding different components through the mixing head, into different designs of molds and placed on a conveyer line (United States of America Patent No. US4424289A, 1984) . There are two major designs of mixer heads, low-pressure dynamic mixing heads and high-pressure dynamic mixing heads (Pilato, 2010). The high-pressure mixing head produces homogenous mixture and finer cell structure than low-pressure mixing head (Pilato, 2010) . Despite the performance, low-pressure mixing head is more commonly used due to lower cost and it also produces substantial amount of foam mixtures in a short duration with a constant quality.

For semi-continuous process, it combines two techniques mentioned above. This technique produces foams with a consistent quality with less investment required (Mougel, Garnier, Cassagnau, & Sintes-Zydowicz, 2019).

2.5.3 Foam morphology and cell density

The morphology or structure of phenolic foam is directly related to mechanical and physical property of its, studying the morphology greatly helps in describing the effect of each parameter on target property. Texture of cell wall, cell size, or cell density are examples of foam morphology that can be studied by using scanning electron microscope (SEM), which is low cost and easy to learn.

Cell density (N_F) represents a number of cell per volume of the foamed polymer. Cell density characterization is performed with the assumption of isotropic distribution of spherical cells (Gosselin & Rodrigue, 2005). The formular used in this project is the cubed square root of number of cell (n) in the micrograph area (A) in cm^2.

$$N_F = \left[\frac{n}{A}\right]^{3/2} \tag{2.1}$$

2.5.4 Thermal conductivity

Thermal conductivity can be defined as the rate of heat transfer through a unit thickness of the material per unit area per unit temperature difference. Thermal conductivity measures the heat conduction capability of a phenolic foam to conduct heat. A high value for thermal conductivity refers to good conductor materials, and low value for thermal conductivity is a poor heat conductor or insulator. Phenolic foam is known as rigid thermosetting polymeric foams with good thermal insulation, high thermal stability, and excellent fire resistance (Ma, 2022) . According to the Fourier's law, the thermal conductivity is defined as:

$$k = \frac{-q}{\nabla T} \tag{2.2}$$

Where q is heat flux (the amount of heat flowing across a unit area per unit time), ∇T refers to temperature gradient. SI unit of thermal conductivity (k) is W/m· K. This equation is appropriate for the steady-state heat conduction. For unsteady-state conduction heat transfer, the element of energy balances is needed to be taken into consideration that the temperature change with the time τ:

$$\rho C_p \frac{\partial T}{\partial \tau} = \frac{\partial}{\partial x}\left(k \frac{\partial T}{\partial x}\right) \tag{2.3}$$

Where ρ is density, C_p is thermal capacity per unit volume of the material. If ρ and C_p are considered to be constant, the non-steady state conduction heat transfer is reduced into: (Ma, 2022)

$$\frac{\partial T}{\partial \tau} = \frac{k}{\rho C_p}\left(\frac{\partial^2 T}{\partial x^2}\right) \tag{2.4}$$

The thermal conductivity of commercial phenolic foam according to EPFA ranges from 0.018 W/m·K depending on national certification requirements.

(Kim & Lee, 2008) prepared phenolic foam with nanometer pore with high strength to investigate effects of pressure and resin concentration that significantly enhance the compressive strength, toughness, thermal insulation properties of phenolic foams result in thermal conductivity of 0.028 W/m·K with the density of 120 kg/m^3. Kim & Lee, 2008 also improved microwave phenolic foaming method based on resole-type phenol-formaldehyde resin using microwave and air

instead of blowing agents results in low density of phenolic foams of 120 kg/m^3 and low thermal conductivity of 0.029 W/m·K for efficient thermal insulation.

2.6 Literature Review

2.6.1 Substitution phenolic monomers into formaldehyde resin

Nasir, et al., 2011 studied the extraction of lignin by kraft and soda pulping process from oil palm empty fruit bunch. The result confirms that a potential active site for polymerization was found in guaiacyl-type (G) unit. Phenol and formaldehyde condense simultaneously in the presence of alkaline to generate methylolphenol in phenol formaldehyde condensation processes. As indicated in Figure, the initial attack might be at the 2 -, 4 -, or 6 -position. The interaction of methylol groups with other accessible phenol or methylolphenol in the second stage resulted in the production of linear polymers, followed by the development of hard cure and highly branching structure. The similarity between the G-type unit of lignin and phenol revealed that G type lignin could also react with formaldehyde and could be cross linked with formaldehyde in the same way as in the phenol formaldehyde condensation reaction polymerization as shown in Fig. As a result, the free 3-position of G-type lignin units yields significant value when compared to S-type lignin unit, which had both the 3-position and 5-position connected to methoxy group, blocking a polymerization process.

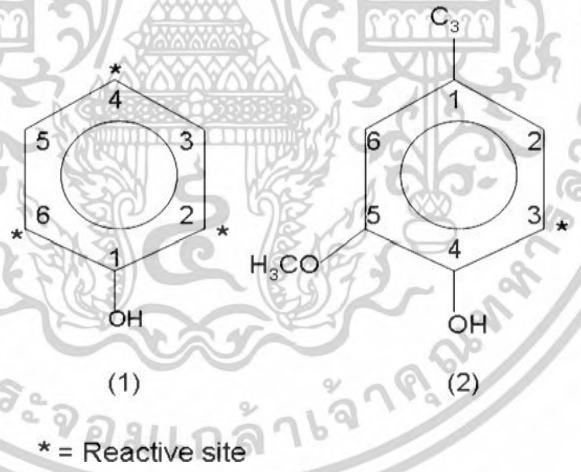

Figure 2.8 (1) Phenol structure with three reactive sites: 2-, 4- and 6-position (2) typical lignin structure with 1 reactive site: 3-position. (Nasir, et al., 2011)

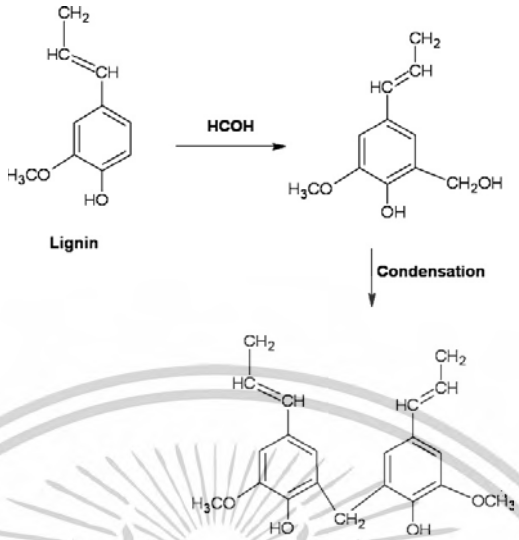

Figure 2.9 Cross-linking between lignin and formaldehyde. (Nasir, et al., 2011)

2.6.2 Two-step depolymerization of sugarcane bagasse lignin under alkaline conditions

Youchang & Srimahaprom, 2021 studied the removal of lignin from the cell wall of sugarcane bagasse as black liquor by hydrothermal liquefaction in first-stage delignification. The reaction conditions, i.e. NaOH solutions of 0.5-12%w/v and temperatures of 100-210°C. In addition, KOH, $Ba(OH)_2$, $Ca(OH)_2$ solutions of 4%w/v and temperature of 140°C were also applied to investigate the effect of alkali types on depolymerization of sugarcane bagasse lignin. The liquefied product from the first stage hydrothermal liquefaction was carried out in second-stage oxidative depolymerization under alkaline conditions to convert lignin to phenolic monomer compounds by using hydrogen peroxide coupled with copper (II) oxide and iron (III) sulfate as catalysts in the second stage at 210-250ºC for sodium hydroxide and at 170-210ºC for other alkalis. The results of the first-stage delignification showed that the optimum condition for removal of lignin from the plant cell wall structure of sugarcane bagasse was the concentration of the sodium hydroxide solution in units of %w/v and temperature in units of °C: (0.5, 210), (1, 200), (2, 180), (3, 160), (4, 140), (5, 140), (6, 130), (8, 120), (10, 110), and (12, 100). In the second stage oxidative depolymerization, the highest yields of phenolic monomers obtained in the range of 10.6-11.5 wt.% at 180-210°C were produced using liquefied lignin obtained from the first stage at 4 %w/v of NaOH with condition of 140-180°C.

The extractives-free sugarcane bagasse was reacted with hydrothermal liquefaction in the first-stage delignification using the optimal conditions for removing lignin from the plant cell wall structure and the liquid product from the first stage is further reacted in the second stage. The liquefied product obtained from this stage is extracted with ethyl acetate and reacted with silylate derivatization with N,O-bis(trimethylsilyl) trifluoroacetamide and pyridine before being analyzed by GC-MS to identify the type and quantity of phenolic monomer compounds that formed.

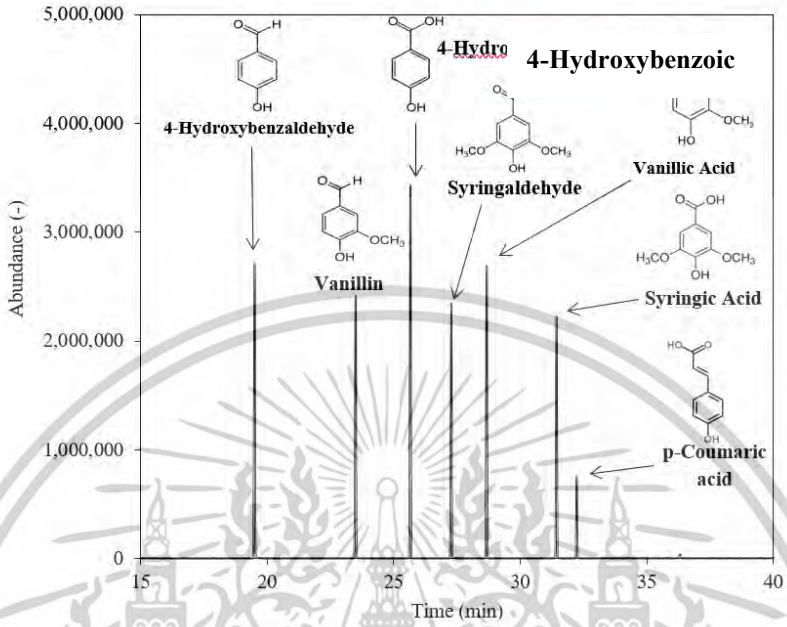

Figure 2.10 Example of GC-MS chromatogram of standard indicating phenolic monomer compounds. (Youchang & Srimahaprom, 2021)

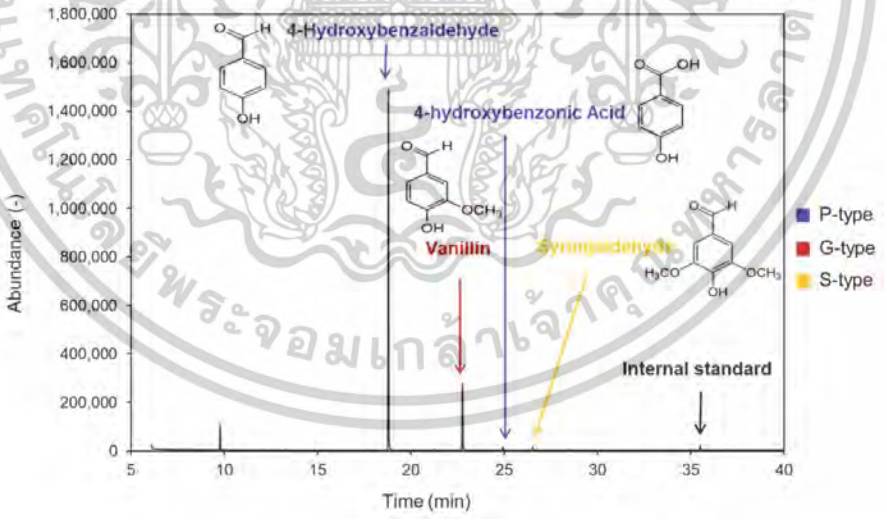

Figure 2.11 Chromatogram of oxidative products by using liquefied lignin from the 1st-stage as treated by 4% w/v NaOH at 140°C and the 2nd-stage at 190°C for 30 min. (Youchang & Srimahaprom, 2021)

The chromatogram shows four main monomer products, i.e. 4-hydroxybenzaldehyde, vanillin, 4-hydroxybennzonic acid, and syringaldehyde. At maximum point, 4-hydroxybenzaldehyde and 4-hydroxybennzonic acid, namely p-type lignin, were found as the main product. The quantitative analysis of phenolic

monomers can be summarized as two-step lignin contains of p-type, g-type, and s-type of 9.7, 1.7, and 0.1 wt.% of macro lignin, respectively.

2.6.3 Characteristics of lignin and phenolic monomer compounds

Youchang & Srimahaprom, 2021 investigated molecular weight of lignin and phenolic compounds from two-step depolymerization of lignin. GPC chromatogram revealed the molecular weight distribution of lignin and phenolic monomer compounds were presented in Figure 2.12 and 2.13 respectively. Lignin and phenolic monomers obtained from one-step and two-step depolymerization of lignin into phenolic monomer compounds exhibited the same trend that was observed in the molecular weight distribution. The weight-average molecular weight (M_w) was below 1,000 Da. However, the weight-average molecular weight obtained in this study is not accurate due to the molecular weight distribution is outside the standard range of 1,013-5,480,000. Therefore, the calculation cannot be compared with the standard.

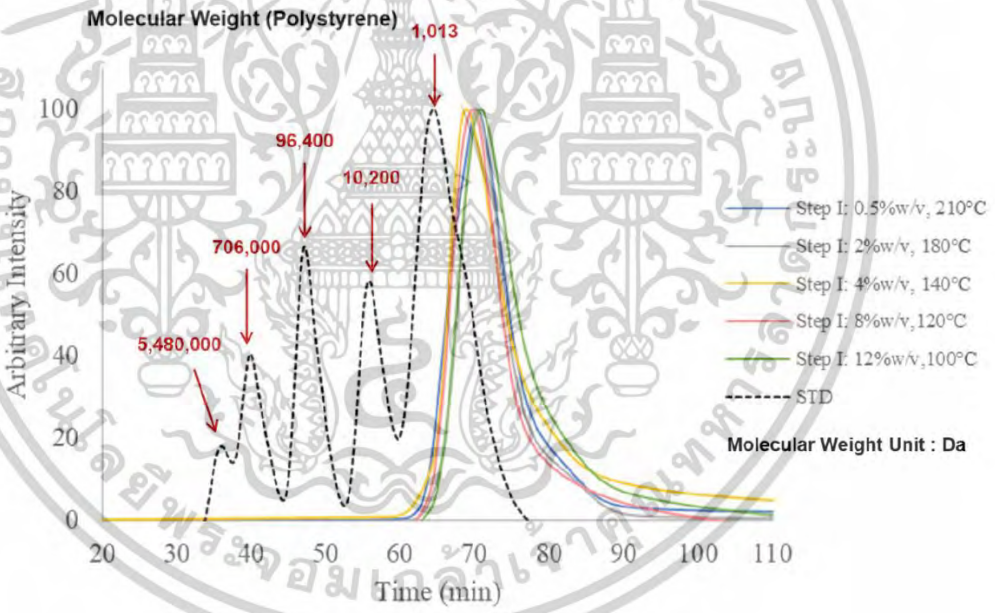

Figure 2.12 Molecular weight distribution of the first-step delignification from sugarcane bagasse, 0.5, 2, 4, 8, and 12%w/v NaOH at 210, 180, 140, 120 and 100°C, respectively. (Youchang & Srimahaprom, 2021)

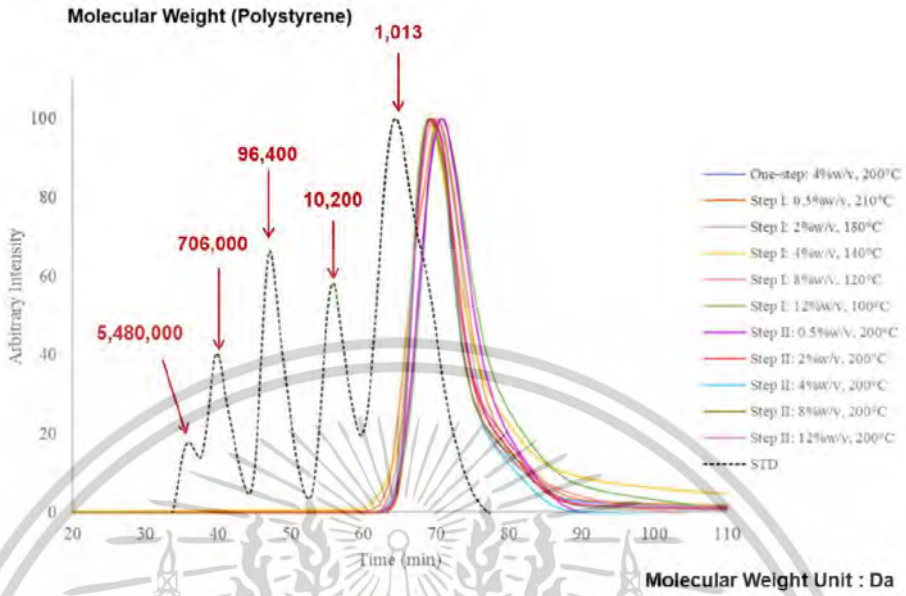

Figure 2.13 Molecular weight distribution of one- and two-step oxidative depolymerization of lignin into phenolic monomer compounds. (Youchang & Srimahaprom, 2021)

2.6.4 New formulations for cost-effective production of bio-based phenol formaldehyde foams with reduced formaldehyde consumption using kraft lignin without any pretreatments

Li, Yuan, Schmidt, & Xu, 2019 generated new foaming formulations for bio-phenol formaldehyde (BPF) resins and thermal insulation foams using kraft lignin for reducing petroleum-based phenol with various recipes results in 50 wt.% highest substitution of lignin and the optimal recipe for foam formulation is obtained by adding blowing agent contains of 5% hexane and 5% pentane mix with tween-80 as an emulsifier and with adding sulfuric acid as a curing catalyst. Obtained closed-cell structure bio foams have low density of 20-80 kg/m^3, strong compressive strength up to 1.01 MPa, high performance of insulation materials with thermal conductivity range of 0.030-0.048 W/m·K, and also provides flame retardant property.

2.6.5 Preparation of bio-based phenol formaldehyde foams using organosolv lignin as a substitute for phenol

Li B. , et al., 2017 produced bio-based phenol formaldehyde (BPF) foams with phenol substitution of 30-50 wt.%. The added lignin obtained from pro-prietary low temperature/low pressure depolymerization process of hydrolysis lignin (DHL, $M_w \approx$ 2000 g/mol). They confirmed that phenol formaldehyde foam and bio-based phenol formaldehyde foam with 30 wt.% substitution have very close in structure including density of 40 kg/m^3, compressive strength of 0.152 MPa, elastic modulus of 2.16 MPa and thermal conductivity of 0.033 W/m/K. In the case of 50% lignin substitution PF foam which provided higher density (108 kg/m^3), higher compressive strength (0.405 MPa) and elastic modulus (7.56 MPa) than the PF foam but thermal conductivity is still as same normal PF foam.

CHAPTER 3
RESEARCH METHODOLOGY

3.1 First-stage hydrothermal liquefaction of extractives-free sugarcane bagasse

Oven-dried extractives-free sugarcane bagasse is used to liquefaction for delignification from lignocellulose under alkaline conditions. The appropriate conditions from (Sinsatitporn, 2019) study are used which is 4 %w/v sodium hydroxide solution and temperature among range 140°C.

3.1.1 Materials and chemicals

1. Oven-dried extractives-free sugarcane bagasse
2. 4 %w/v of sodium hydroxide solution
3. 99.99 wt.% nitrogen gas

3.1.2 Equipment and apparatus

1. Autoclave Parr reactor with capacity of 1.5 L
2. Vacuum filter
3. Filter paper (PTFE membrane, 0.45 μm)
4. 1-mL glass pipette
5. Iced-water bath

3.1.3 Experimental procedure

1. Load 20 g of extractives-free sugarcane bagasse into the batch reactor.
2. Add 1 L of sodium hydroxide solution into batch reactor. Tighten the reactor cap then pressurize with nitrogen gas at 2.5 MPa and check leakage.
3. Install the autoclave reactor to heater (furnace) and controller board, set the desired temperature of 140°C, and switch on the system.
4. Let the reaction undergo for 30 min, then cool the reactor temperature down by quenching in iced-water bath for 30 min.
5. Release pressurized nitrogen in the reactor by gently open the reactor valve.
6. Open a reactor and filter the mixture by vacuum filtration.
7. Collect the filtrates for the second-stage experiment.

3.2 Second-stage oxidative depolymerization of liquefied lignin to phenolic monomers

3.2.1 Materials and chemicals

1. Liquefied portion from the first-stage hydrothermal liquefaction (section 3.1.1)
2. 30 wt.% of hydrogen peroxide
3. Copper (II) oxide
4. Iron (III) sulfate

5. 0.05 mg/mL of 1,3-diphenoxybenzene in ethyl acetate
6. 72 wt.% of sulfuric acid
7. 99.99 wt.% nitrogen gas

3.2.2 Equipment and apparatus

1. Autoclave reactor with capacity of 1.5 L
2. Vacuum filter
3. Filter paper (PTFE membrane, 0.45 μm.)
4. 1-ml glass pipette
5. Iced-water bath

3.2.3 Experimental procedure

1. Load 800-980 mL of liquefied portion from the first-stage, 40 g of copper (II) oxide, and 4 g of iron (III) sulfate into the reactor.
2. Add 80 mL of hydrogen peroxide into autoclave reactor. Tighten the reactor cap and check leakage by pressurizing it with nitrogen gas (2.5 MPa).
3. Install the autoclave reactor to furnace, set the desired temperature of 190°C, and switch on the system.
4. Let the reaction undergoes for 30 minutes, then cool the reactor temperature down by quenching in in iced-water bath for 30 minutes.
5. Release pressurized nitrogen in the reactor by gently opening the reactor valve.
6. Open a reactor and filter the mixture by using a vacuum filter.
7. Neutralize the filtrate with 72 wt.% of sulfuric acid.
8. Extract the obtained filtrate with ethyl acetate.

3.3 Extraction of lignin compounds

3.3.1 Materials and chemicals

1. Neutralize liquefied portion from hydrothermal liquefaction
2. Ethyl acetate

3.3.2 Equipment and apparatus

1. 1-mL glass pipette
2. Pasteur pipette
3. 5 ml test tube

3.3.3 Experimental procedures

1. Load 200 ml of neutralize liquefied into separating funnel.
2. Add 15ml of ethyl acetate into separating funnel.
3. Tighten the separating funnel and shake it by hand then left to settle the solution and acetate into different layers.
4. Wait for lignin to diffuse into ethyl acetate layer and open valve to take the yellow solution out from separating funnel.
5. Collecting ethyl acetate layer into the beaker and let it dry in vacuum hood.
6. When lignin and salt was crystallized, grind or crack it into powder.
7. Dissolve the powder in water then pours it into centrifugal tube.

8. Set centrifugal speed to 8000 rpm and start, after finished take out the solution and measure pH with pH indicator, fill the water to the tube and repeat to procedure for minimum 8-13 times.
9. After repetition, take the water out and remain it at low level to ensure lignin presence and agitate leftover into suspension solid form and take it into beaker, then let dry in vacuum hood.

3.4 Synthesis of phenol-formaldehyde resin

For synthesis, phenol-formaldehyde (PF) resin type depends on the molar ratio of phenol to formaldehyde and the mode of catalyst. We chose to synthesize the resole resin, with ratio of F/P of 2 and basic catalysts, due to resole resin has various applications when compared with novolac resin.

3.4.1 Materials and chemicals

1. 99.6% phenol AG for analysis
2. 10 %w/v of sodium hydroxide solution
3. 37 wt.% of formaldehyde solution
4. 99.6% methanol AG for analysis

3.4.2 Equipment and apparatus

1. 250-mL three necks round bottom flask with reflux condenser
2. Thermometer
3. Hot plate and stirrer with magnetic bar
4. Stand and cramp
5. 25-mL Beaker
6. Oil bath
7. Micropipette

3.4.3 Experimental procedures

1. Load 9.8 mL of formaldehyde solution 37 wt.% and phenol 6.20 g into three necks round bottom flask.
2. Drop the sodium hydroxide 2.4 mL into three necks round bottom flash.
3. Set hot plate, stirrer and put magnetic bar into three necks round bottom flash with reflux condenser.
4. Put the three necks round bottom flash with condenser on the magnetic stirrer and let it stir with magnetic bar and maintain temperature at 80 - 90ºC for 1 hr.
5. Pour the product out of the three necks round bottom flask into beaker.

3.5 Determination of crosslinking degree of PF resin

The experiment to investigate crosslinking degree was conducted as reflux with xylenes following ASTM D2765 standard test methods for determination of gel content and swell ratio of crosslinked plastics. This was done to study the optimal time of phenolic resin reaction time. The results were then used in synthesizing all formular.

3.5.1 Materials and chemicals

1. Xylenes AG for analysis, boing point of 138 to 141ºC.
2. 2,2'-methylene-bis (4-methyl-6-tertiary butyl phenol) as an antioxidant

3.5.2 Equipment and apparatus

1. 250 mL Round-bottom flask, with large-mouth ground-glass or cork joint.
2. Heating mantle
3. Reflux condenser
4. Ring stand and appropriate clamps
5. Drying oven

3.5.3 Experimental procedures

1. Put the PF resin in drying oven to cure the resin as a solid plastic at 70ºC for a day.
2. Weigh the weight of sample (W_1).
3. Set up the apparatus as shown in figure 3.1.
4. Prepare xylenes 180 mL in round-bottom flask.
5. Dissolve 1.5 g (1 wt.% of xylene) antioxidant in xylene to inhibit further crosslinking of sample and put the sample into round-bottom flask.
6. Adjust reflux ring of xylenes in reflux apparatus.
7. Let the reaction undergo for 12 hours.
8. Remove the sample from round-bottom flask.
9. Put the sample in drying oven to dry the remaining xylenes on the sample at 150 ºC for a night.
10. Weigh the weight of sample (W_2).

3.5.4 Calculation of crosslinking degree

$$\text{Crosslinking degree} = \frac{W_2}{W_1} \times 100\ \% \qquad (3.1)$$

Where W_1 is the weight of cured sample before reflux.

W_2 is the weight of cured sample after reflux.

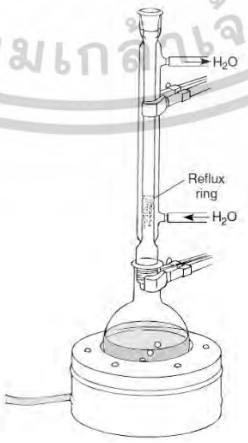

Figure 3.1 Reflux apparatus for macroscale reactions, using a heating mantle and water-jacketed condenser (Pavia, Kriz, Lampman, & Engel, 2015).

3.6 Synthesis of LPF resin

In LPF resin synthesizing, the condition, equipment, and procedure used were similar with the synthesis of phenolic resin, but with the difference of substitution of phenol with extracted lignin 10 and 50 wt.% of phenol used in phenolic resin to study the effects of lignin addition to the foam properties.

3.6.1 Materials and chemicals

1. 99.6% phenol AG for analysis
2. 10 %w/v of sodium hydroxide solution
3. 37 wt.% of formaldehyde solution
4. 99.6 % methanol AG for analysis
5. Solidified lignin from hydrothermal liquefaction (first-step lignin and second-step lignin)

3.6.2 Equipment and apparatus

1. 250-mL three necks round bottom flask with reflux condenser
2. Thermometer
3. Hot plate and stirrer with magnetic bar
4. Stand and cramp
5. 25-mL Beaker
6. Oil bath
7. Micropipette

Figure 3.2 Reflux setup for phenol-formaldehyde (PF) or lignin-phenol-formaldehyde polymerization.

3.7 Foaming the LPF foams

The foaming process involved mixing of the lignin-phenol-formaldehyde (LPF) resin, blowing agent, surfactant, and curing catalyst.

3.7.1 Materials and chemicals

1. n-pentane AG for analysis as a blowing agent
2. Tween-80 as a surfactant
3. 72 wt.%. sulfuric acid as a curing foam catalyst

4. Drying oven
5. Disposal molds with dimensions of 5x5x1 cm.

3.7.2 Experimental procedures

1. Mix LPF or PF resin with 1.2 g Tween-80 and 4 g of n-pentane in the mold then mix vigorously at room temperature as a viscous solution.
2. Slowly drop 2.2 mL of 72 wt.%. sulfuric acid into the viscous solution under vigorous agitation for 30 seconds at room temperature.
3. Transfer the viscous solution into drying oven for curing a foam at 70 ºC for 30 minutes.
4. Cut each sample into dimensions of 5x5x1 cm. by using cutting saw.

3.8 Scanning Electron Microscope (SEM) characterization

SEM is a test process that scans a sample with an electron beam to produce a magnified image for analysis. It is used to examine external morphology and pore size of foams.

3.8.1 Materials and chemicals

1. Gold sputter coater
2. Scanning electron microscope (SEM) EVO MA10

3.8.2 Experimental procedures

1. Before SEM characterization, samples must be cut into 1x1x1 cm and dried to eliminate any outgassing from organic contamination and water.
2. Deduct and shape the sample to an appropriate size for SEM characterization.
3. Coat the sample by using gold sputter coater to have a conductive surface.
4. Bring the sample to characterize by SEM.
5. Bring the results from SEM to analyze with ImageJ to examine foam morphology and its pore size.

3.9 Density of Foams

Foam density is measured by using electronic densimeter MD-200S and the density results will be compared with commercial phenolic foams.

3.10 Cell Density of Foams

Cell density of each sample were determined by counting the number of foam cells per area obtained from SEM images.

$$\text{Cell density (cells/cm}^3) = \frac{\text{numbers of foam cells}}{\text{scaning area from SEM image}} \qquad (3.2)$$

3.11 Thermal conductivity

Thermal conductivities of foams were determined by applying ASTM C518 for bulk material under steady-state model (Zhao, Qian, Gu, Jajja, & Yang, 2016)

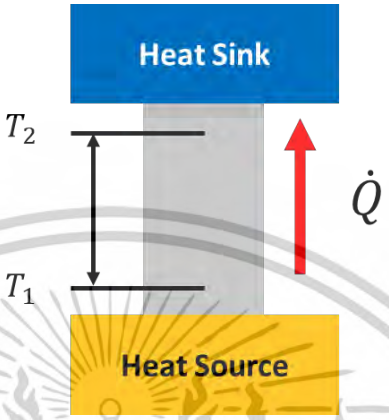

Figure 3.3 Schematic of steady-state model for measuring thermal conductivity of the materials.

In steady-state heat transfer measurement, thermal conductivity is determined by measuring temperature gradient (ΔT) at wall thickness. The sample is placed between the heat source and heat sink as shown in fig. The temperature is measured by using thermocouples due to its accuracy and availability [ref measurement technique]. Thermal conductivity can be calculated using Fourier's law of heat conduction.

$$k = \frac{\dot{Q}L}{A\Delta T}$$

$$\dot{Q} = \dot{Q}_{Actual} - \dot{Q}_{loss}$$

Where $\dot{Q}$ is the amount of heat flowing through the sample (W/m·K), A is the cross-sectional area of a sample (m^2), L is the distance between measuring T_1 and T_2, $\dot{Q}_{Actual}$ is applied heating power at heat source side, and $\dot{Q}_{loss}$ is the heat losses from natural convection and radiation to ambient including conduction through thermocouple wires. Unfortunately, conduction heat transfer from sample through thermocouple wire is difficult to measure. Therefore, the assumption of neglect of heat transfer through the wire is required.

CHAPTER 4
RESULTS AND DISCUSSION

In this chapter, the results were discussed in effect of lignin substitution from first and second-stage lignin from sugarcane bagasse to synthesize phenol foams (4.1) First and second-stage delignification yields, (4.2) Crosslinking degree of PF resin, (4.3) morphology of PF, LPF, and KLPF foams (4.4) density of PF, LPF, and KLPF foams, and (4.5) thermal conductivity of PF, LPF, and KLPF foams.

4.1 First and second-stage delignification yields

Yields of lignin in 1st-stage and 2nd-stage delignification were recorded throughout every batch. Weights of sugarcane bagasse were recorded before and after undergoing delignification with weight of obtained lignin to calculate the yield of lignin with loss during lignin isolation.

Table 4.1 Yield of lignin obtained from 1st-stage delignification.

Batch No.	Weight of dry bagasse (g)	Weight of delignified bagasse (g)	Obtained 1st-stage lignin (g)	Weight loss (g)	Yield (%)
1	20.00	16.12	3.74	0.14	18.70
2	20.00	15.46	4.16	0.38	20.80
3	20.00	15.59	4.36	0.05	21.80
4	20.00	15.52	4.24	0.24	21.20
5	20.00	15.40	4.52	0.08	22.60
6	20.00	15.16	4.12	0.72	20.60

The total lignin obtained from 1st-stage delignification was 25.14 g from 120 g of sugarcane bagasse, which is 20.95 %yield. The average lignin from each batch was 4.19 ± 0.26 g with average loss of 0.27 ± 0.25 g. The loss of mass refers to hemicellulose attached with lignin during delignification, which can normally occur, and remain in water after purification.

Table 4.2 Yield of lignin and monomers obtained from 2nd-stage delignification.

Batch No.	Obtained lignin with monomers (g)	Yield (%)	Lignin (g)	Lignin monomers (g)
1	4.12	20.60%	3.71	0.41
2	3.99	19.95%	3.59	0.40
3	4.05	20.25%	3.65	0.41
4	4.02	20.10%	3.62	0.40

The total lignin and monomers obtained from 2nd-stage delignification was 16.18 g with 14.56 and 1.62 g of lignin and lignin monomers respectively. The amount of lignin monomers was estimated using previous study results with lignin monomers obtained for 10 wt.% of lignin. The average lignin monomers per batch was 0.40 ± 0.05 g.

4.2 Crosslinking degree of PF resin

The sample of PF resin was used to study crosslinking degree with different reaction time (30, 60, 90, 120 minutes) to estimate reaction completion. Each reaction time was repeated 3 times. The results were displayed as shown in Figure 4.1 to demonstrate how reaction time affects polymerization reaction.

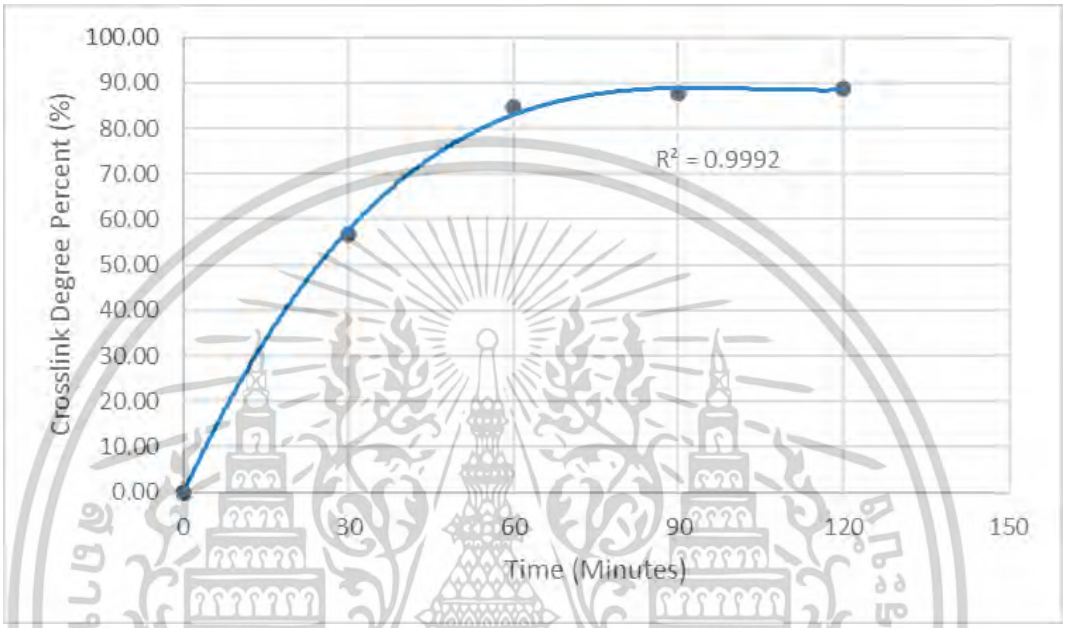

Figure 4.1 Crosslinking degree on different reaction times.

From Figure 4.1, the reaction reaches maximum crosslinking degree of 87.83% at 90 minutes. Further reaction did not increase crosslinking degree with 120 minutes of reaction time, the crosslinking degree reach 88.67% which indifferent from 120 minutes. The crosslinking degree was 56% and 81.33% for 30 and 60 minutes respectively. Since the reaction approaching maximum crosslinking at the time of 60 minutes, the reaction time of 60 minutes was used in all resin synthesizing.

4.3 Morphology of PF and LPF foams

Each foam sample of PF, 1st-stage (1-LPF-10% and 1-LPF-50%) and 2nd-stage LPF (2-LPF-10% and 2-LPF-50%), and KLPF foam (KLPF-10% and KLPF-50%) was examined using EVO MA10 scanning electron microscope (SEM) to investigate the morphology and pore diameter on the surface of the foam. The pore diameter was then used to calculate cell density (N_F). The results were displayed in Figure 4.5 to show trend of effects.

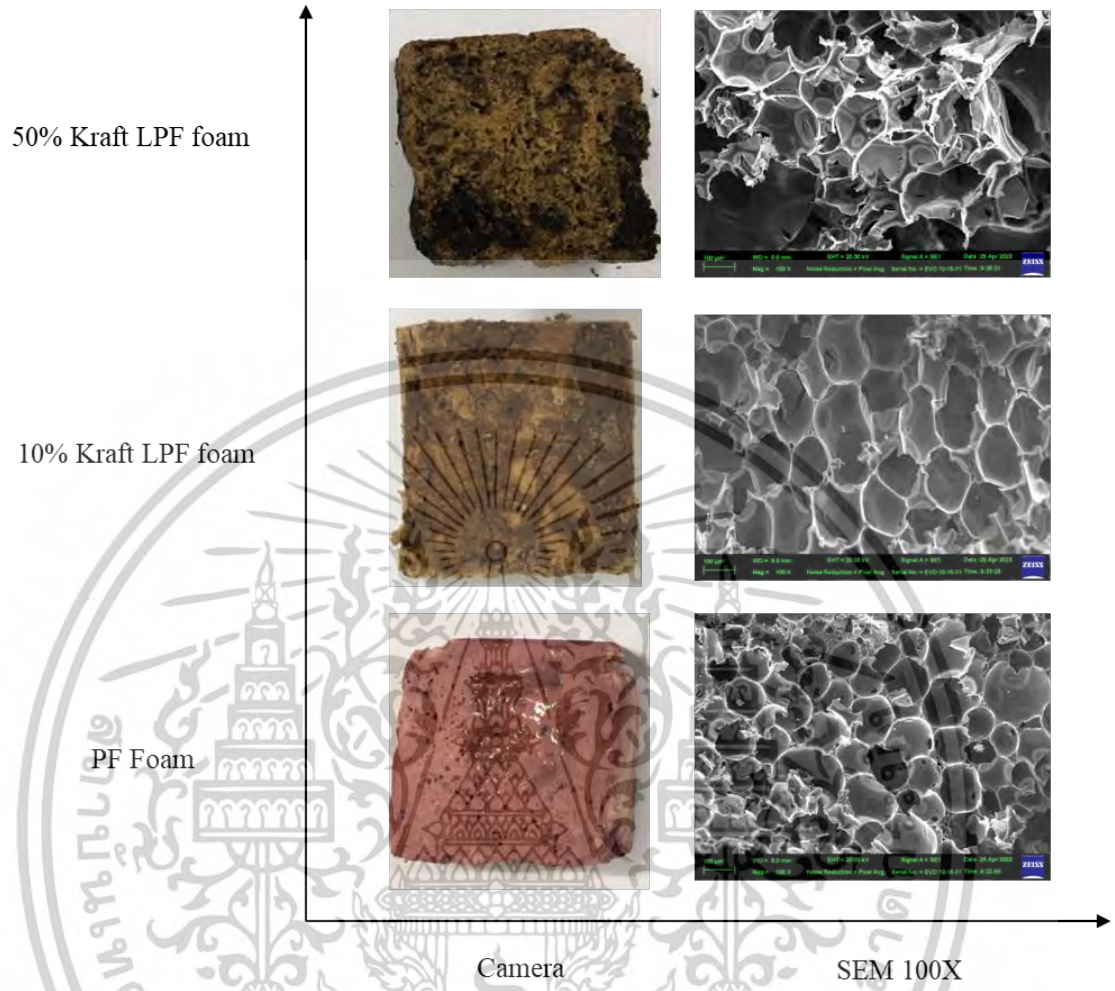

Figure 4.2 Representative SEM images of PF and kraft LPF foams.

Representative pictures of phenolic foams in Figure 4.2. The pink color foam is 100% PF foam or conventional PF foam, while others are 10% and 50% kraft LPF foam which have dark brown color for both substitutions. The cell structure of PF and kraft LPF foam were observed by SEM as shown in Figure 4.2. All the foams, the cells are mostly closed cells, even though there are some perforations by the presence of water as a by-product from polymerization (Li B. , et al., 2017) . The ruptures and debris appear in all foams from SEM sample preparation. PF foam has relatively more uniform cell size and shape than 1st-stage LPF foams. The reason of bigger cell size is the increasing of surface tension from addition of lignin, rich in hydroxyl group, which causes difficulty in bubble entrapping during the foaming process, leading to bigger cells. Moreover, the open cells obtained due to lower structural strength of polymer chain.

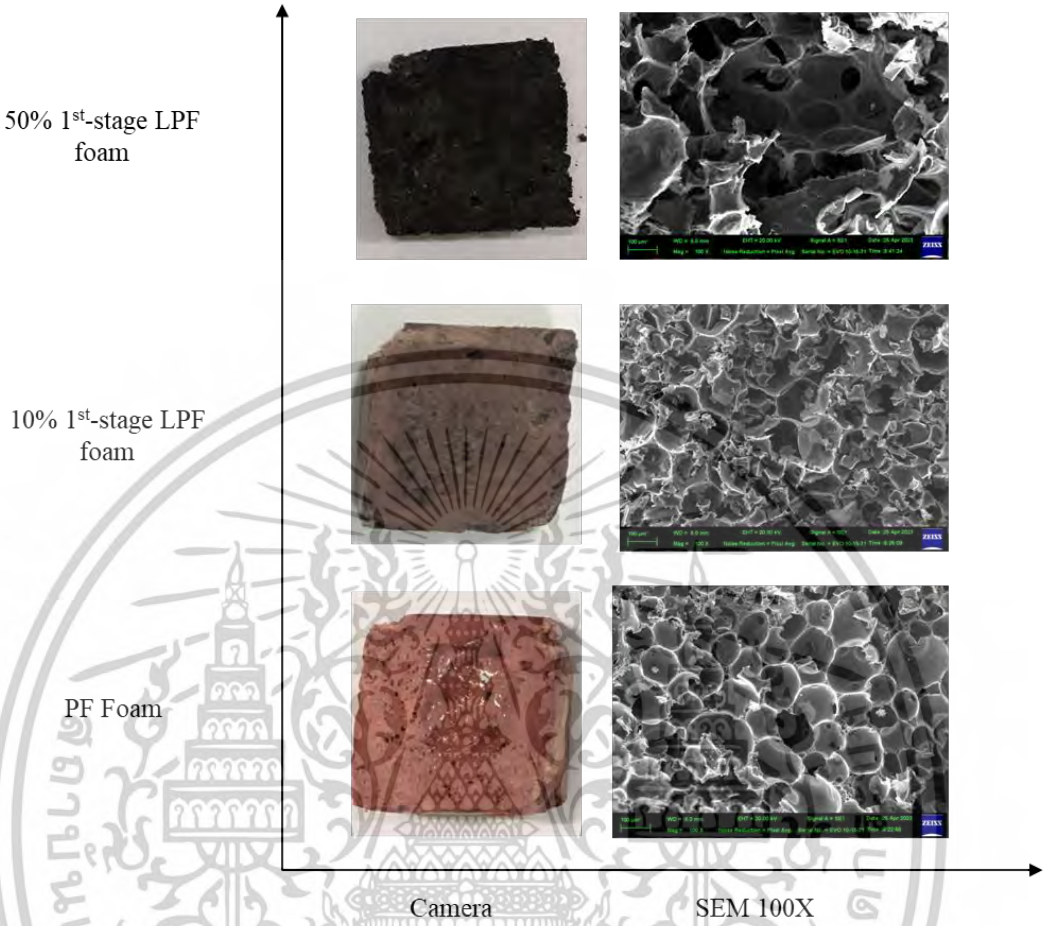

Figure 4.3 Representative SEM images of PF and 1st-stage LPF foams.

Representative pictures of phenolic foams in Figure 4.3. The pink color foam is 100% PF foam or conventional PF foam, others are 10% and 50% 1st-stage LPF foam which have dark brown to black color, respectively. The cell structure of PF and 1st-stage LPF foam were observed by SEM as shown in Figure 4.3. 1st-stage LPF foams have similar cell structure to kraft LPF foams but contain more open cells when lignin 50 wt.% substitution is reached. PF foam has relatively more uniform cell size and shape than 1st-stage LPF foams. The reason of bigger cell size is as same as in kraft LPF discussion that the larger molecule of 1st-stage lignin than petroleum phenol increases surface tension of the resin which rich in hydroxyl group makes 1st-stage LPF resin difficult to entrap the foaming process, leading to bigger cells obtained along with open cells in 50% 1st-stage LPF foam.

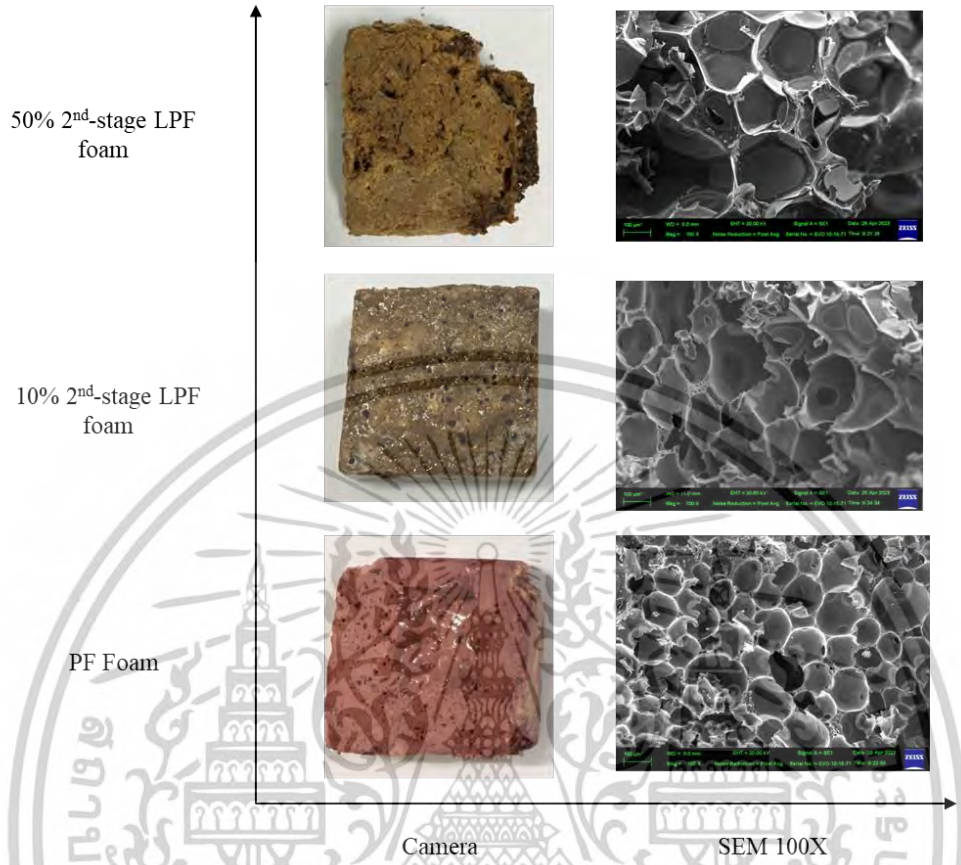

Figure 4.4 Representative SEM images of PF and 2nd-stage LPF foams.

Figure 4.4 shows representative SEM images of PF and 2nd-stage LPF foams. It can be seen that the 2nd-stage foams exhibit brown color and cells of all foams are mostly closed. The perforations including ruptures or debris are also contained in foam. The 10 wt.% and 50 wt.% 2nd-stage LPF foam provide bigger cell size than PF foam that had been discussed before. This is probably due to the surface tension of the resin and weaker structural strength of lignin that was added to LPF resin cannot withhold bubble growth. For 50 wt.% 2nd-stage LPF foam provides the biggest cell size of all resulted foams. This is the result of the addition of lignin and monomers which affects the polymer chain size and weakens structural strength of its chain.

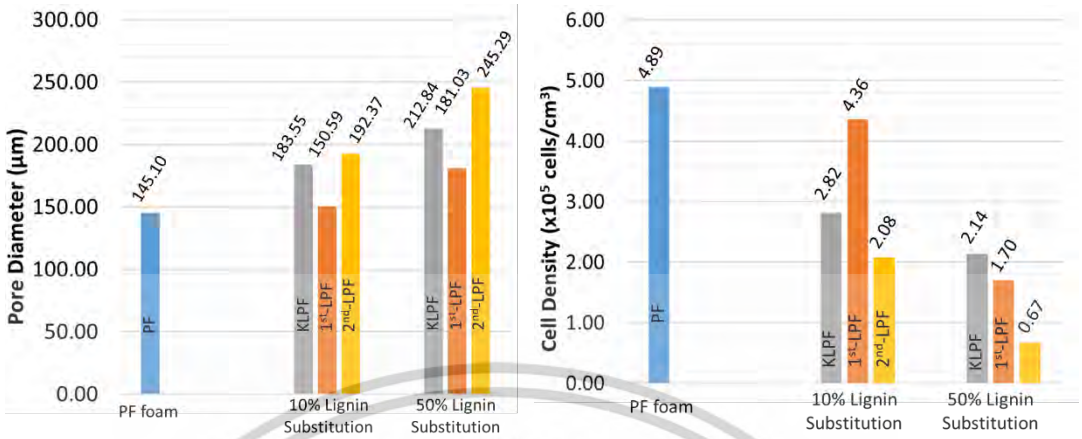

Figure 4.5 Pore diameter (left) and cell density (right) of different lignin substitution.

The pore diameter of PF foam was 145.10 µm, which was used as reference to study the effects of lignin substitution. When kraft lignin was used as substitution in phenolic foam, pore diameter was increased to 183.55 and 212.84 µm for 10 wt.% and 50 wt.% substitution respectively. The increased diameter is due to the bigger molecular structure of lignin which enlarges overall KLPF polymer structure. With more substitutions, the pore diameter is bigger due to the same reason as mentioned before. When 1st-stage lignin was used, the pore diameter was 150.59 and 181.03 µm for 10 wt.% and 50 wt.% accordingly. The overall pore diameter of 1st-stage LPF foam was lower than KLPF foam. This was expected since 1st-stage lignin was isolated using alkali method resulting in no presence of sulfur in structure while kraft lignin had low presence of sulfur. The sulfur in structure might cause weakening structural strength resulting in larger pore due to weaker capability to withhold bubble growth include surface tension effect when compare the structure between kraft and 1st-stage lignin, it can infer that interaction of hydrogen bonds in kraft lignin is higher than 1st-stage lignin results in the higher surface tension and the bigger pores generated. Pore diameter from 2nd-stage lignin substitutions were significantly larger than 1st-step lignin with 192.37 and 245.29 µm for 10 wt.% and 50 wt.% respectively. Lignin monomers in 2nd-stage lignin might be the causes of weaker structural strength of resin including the stronger surface tension effect from hydrogen bonding interactions of the big and small molecule, resulting in larger gas bubble during bubble growth thus bigger pore.

The pore diameters as mentioned above were then used to calculate cell density of each foam formulation. The cell density is reversely proportional to pore diameter of foam due to the calculation method. Phenolic resin has the highest cell density of 4.89×10^5 cells/cm^3 due to smaller pore diameter resulting in more amount of pore per area of foam. When considering 10% phenol substitution, 1st-stage lignin has highest cell density among all substitution with 4.36×10^5 cells/cm^3 followed by 2.82×10^5 cells/cm^3 and 2.08×10^5 cells/cm^3 for kraft and 2nd-stage lignin respectively. These results support idea of impacts from lignin molecule's structure to surface tension, the higher surface tension generates big pores of the foam which made

difficulty bubble formation. For 50% substitution, the results are 1.70×10^5 cells/cm^3, 2.14×10^5 cells/cm^3, and 0.67×10^5 cells/cm^3 for 1st-stage, kraft, and 2nd-stage lignin respectively. Result trend of 1st-stage and kraft lignin contradicts with results in 10% substitution, with 1st-stage LPF foam has slightly lower cell density. This is probably due to the higher amount of lignin in LPF and KLPF make overall resin structure indifferent to each other. In contradiction, 2nd-stage LPF foam has significantly lower cell density due to the result of fixing other chemicals and condition to be constant in every foam formular which might not be suitable with the presence of lignin monomers with macro structure lignin. The effects of lignin monomers of 2nd-stage lignin to resin polymerization reaction must be investigated further to give a clear answer of this result.

4.4 Density of PF and LPF foams

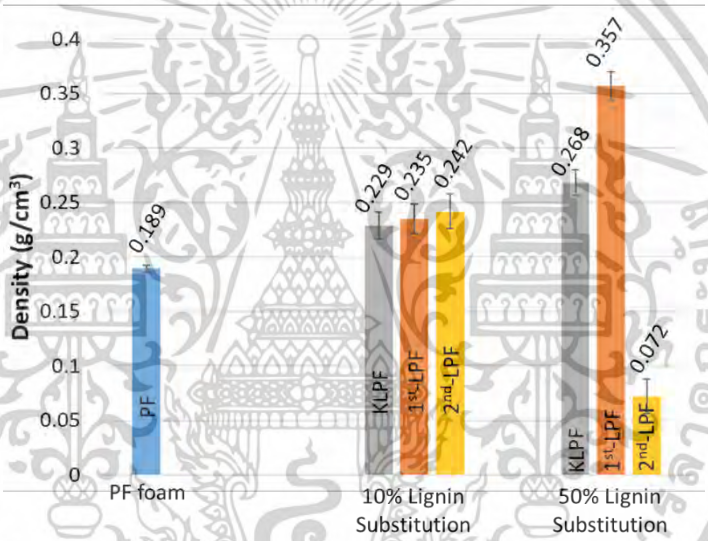

Figure 4.6 The apparent density of phenolic foams with different lignin substitutions.

The apparent densities of all foams were determined by using electronic densimeter found that the phenol formaldehyde foam has a density of 0.189 g/cm^3 corresponds with commercial phenolic foam which has range of density from 0.035-0.200 g/cm^3 according to EPFA.

Figure 4.6 reveals the tendency of foam density on 10% lignin substitution, for 1st-stage and kraft lignin, the density of resulted foam increases with increasing amount of lignin (0.229 g/cm^3 for kraft lignin and 0.235 g/cm^3 for 1st-stage lignin). The reason for the increasing density is macro structure of lignin in resin results in increasing of resin average molecular weight. Thus, the increased amount of lignin in resin structure results in higher density. The same trend can be observed in 50% substitution with 0.268 and 0.357 g/cm^3 for kraft and 1st-stage lignin respectively. The increased in difference is probably due to difference in macro molecule structure of kraft and 1st-stage lignin, with kraft lignin having sulfur element in lignin chain might result in less resin polymerization reaction.

For 2nd-stage lignin, 10 wt.% lignin substitutions in phenol provides enormous LPF foam density of 0.242 g/cm^3. The result is following the trend of kraft and 1st-stage lignin, which was same reason as mentioned before. However, with 50% substitution, the density of 2nd-stage LPF foam decreased significantly to 0.072 g/cm^3. Though reasons behind this feature are not concluded yet, one possible reason is the formular of resin synthesizing. The large presence of lignin monomers might cause the change in overall reaction leading to no polymerization reaction. To know the reason behind this feature, the study of LPF resin reaction with presence of lignin monomers must be conducted in future study.

4.5 Thermal conductivity of PF and LPF foams

Thermal conductivity is an important property of thermal insulation materials for energy storage in cryogenic and refrigeration applications. All the resulted foams have thermal conductivity range of 5.530-9.670 W/m·K. However, the results deviate from foam property that have too high thermal conductivity due to the used technique in order to determine thermal conductivity has major challenges to determine heat flow rate ($\dot{Q}$) through the samples where the heat losses contain of convection and radiation to surrounding and conduction through thermocouple wires and measure temperature accurately. As a result, thermal conductivities of PF and LPF foams are not exactly correct in this experiment (Zhao, Qian, Gu, Jajja, & Yang, 2016)

As shown in Figure 4.7, conventional PF foam has a thermal conductivity of 9.67 W/m·K which is not followed as mentioned before. For kraft ,1st-stage, and 2nd-stage LPF foam, the tendency of thermal conductivities is the same for all foam when substitute lignin up to 50 wt.%. The higher the amount of substituted lignin, the lower thermal conductivity of the foams. The main reason is the lower reactivity of lignin in LPF resin that generated low crosslink density that made bubble coalescence occur during foam formation, leading to enlarged pores trapping air inside. As a result, the bigger pores provide lower thermal conductivity.

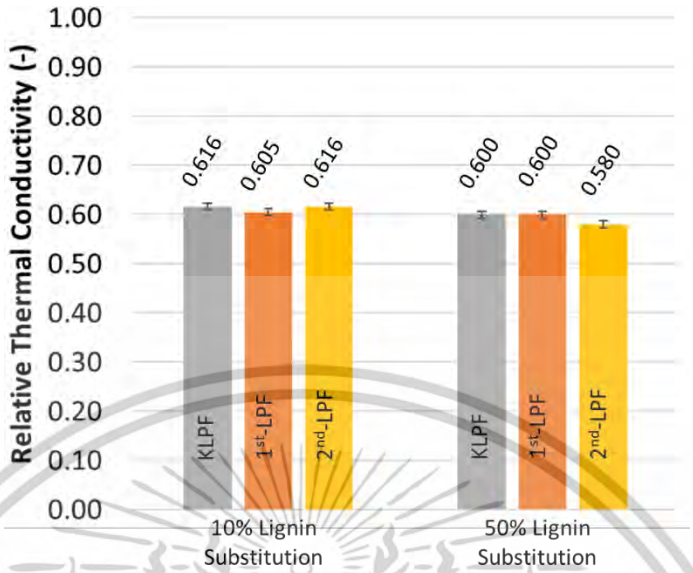

Figure 4.7 Relative thermal conductivity of LPF foams with different lignin substitutions to PF foam.

CHAPTER 5
CONCLUSION AND RECOMMENDATION

5.1 Conclusion

The objectives of this research are to synthesize insulation foam from lignin-phenol-formaldehyde (LPF) resin using liquefied lignin obtained from sugarcane bagasse and study trend of foam's thermal property and structure after replacing phenol with lignin.

Synthesized resin including PF, KLPF, 1st-stage LPF, and 2nd-stage LPF resin with 10 and 50 wt.% substitution can be used to produce thermal insulation foam. With PF, and KLPF foam as reference and comparison for 1st-stage and 2nd-stage lignin foam. KLPF and 1st-stage LPF foam can be produced at both 10% and 50% substitution following with previous research (Li, Yuan, Schmidt, & Xu, 2019). Pore diameter, Cell density, and density of these foams exhibit normal trend with no strange result. However, 2nd-stage LPF foam exhibits strange results in 50% substitution. The foam pore diameter is significantly larger than other foam in our research with very low cell density. The density of the foam is also very low compared to other foams. This feature might be caused by inappropriate formulation due to effects of the presence of lignin monomers on resin polymerization reaction. Further investigation on resin polymerization with 2nd-stage lignin is suggested to be studied.

Thermal conductivity of synthesized foam exhibits great trend when lignin is present though increasing in lignin replacement do not decrease thermal conductivity proportionally. Results show no difference between each replacing lignin, KLPF, 1st-stage and 2nd-stage LPF has almost identical thermal conductivity.

5.2 Recommendation

5.2.1 Method of lignin compounds isolation

The extraction of lignin compounds with ethyl acetate do not isolate efficiently. Repetition must be done, in both 1st-stage and 2nd-stage, to acquire high yield of lignin compounds. The isolation method should be revised to be more efficient for sufficient amount of lignin to conduct experiment effectively. The most commonly used method of acid precipitation should be studied of any effects on lignin structure if used.

5.2.2 Synthesis of lignin-phenol-formaldehyde resole resin

Since lignin and lignin monomers molecular structure is not exactly same as phenol molecule, with the present of macro molecule and less reactive molecule causing effects on polymerization reaction. Further study on adjusted resole resin formular must be done. Addition of solvent and adjusting the ratio of formaldehyde and sodium hydroxide is suggested to be investigated.

5.2.3 Determination of LPF resin crosslinking degree

In this research, only crosslinking degree of PF resin had been conducted. To study the effects of phenol replacement with lignin completely, investigation on resin completion should be done to analyze foam structure with sufficient information.

5.2.4 Foaming formulation

The formulation of foam used in this research is based on previous study (Mougel, Garnier, Cassagnau, & Sintes-Zydowicz, 2019) . The optimization of formulation should be done to apply with foam in this research since 2^{nd}-stage lignin has not been studied before. The best conditions of foaming formulation should be applied to achieve discussable results.

5.2.5 Determination of foam thermal conductivity

Thermal conductivity determination of this research is done according to ASTM C518 without proper equipment. The determination should be done with proper test equipment by sending it to National Metal and Materials Technology Center or Department of Science Service. The samples must be prepared before being sent to undergo testing, with proper size and number of samples.

REFERENCES

Anantkijthamrong, A. (2016). Conversion of Lignin to Phenolic Monomers under Alkaline Conditions by using Hydrogen Peroxide with Copper (II) Oxide and Iron (III) Sulfate Catalysts.

B. Kamm, M. Gerhardt, G. Dautzenberg. (2013). Catalytic Processes of Lignocellulosic Feedstock Conversion for Production of Furfural, Levulinic Acid, and Formic Acid-Based Fuel Components. In New and Future Developments in Catalysis (pp. 91-113). Elsevier.

Caihong, W., Xiaowei, P., & Yejun, H. (2021). Depolymerization and conversion of lignin to value-added bioproducts by microbial and enzymatic catalysis. Biotechnology for Biofuels, 14-84.

Çengel, Y. A., & Ghajar, A. J. (2014). Heat and mass transfer: Fundamentals and applications (5th ed.). New York: McGraw-Hill Professional.

Daothong, P., & Yingsirisit, N. (2021). Synthesis of bioplastic from lignin of sugarcane bagasse.

G. Calvo-Flores, F., A. Dobado, J., Isac-Garcia, J., & J. Martin-Martinez, F. (2015). What is Lignin? In Lignin and Lignans as Renewable Raw Materials (pp. 11-41). John Wiley & Sons, Ltd.

Gardziella, A., Pilato, L. A., & Knop, A. (2000). Phenolic Resins: Chemistry, Applications, Standardization, Safety and Ecology. New York: Springer.

Gosselin, R., & Rodrigue, D. (2005). Cell morphology analysis of high density polymer foams. Polymer Testing, 1027-1035.

Grishechko, L. I., Amaral-Labat, G., Szczurek, A., Fierro, V., Kuznetsov, B. N., & Celzard, A. (2018). Lignin-phenol-formaldehyde aerogels and cryogels. Microporous and Mesoporous Materials, 19-29.

Guo, D.-l., Wu, S.-b., Liu, B., Yin, X.-l., & Yang, Q. (2012). Catalytic effects of NaOH and Na2CO3 additives on alkali lignin pyrolysis and gasification. Applied Energy, 22-30.

Landrock, A. H. (1995). Handbook of Plastic Foams. New Jersey: Noyes Publications.

Li, B., Wang, Y., Mahmood, N., Yuan, Z., Schmidt, J., & Xu, C. C. (2017). Preparation of bio-based phenol formaldehyde foams using depolymerized hydrolysis lignin. Industrial Crops and Products, 409-416.

Li, B., Yuan, Z., Schmidt, J., & Xu, C. C. (2019). New foaming formulations for production of bio-phenol formaldehyde foams using raw kraft lignin. European Polymer Journal, 1-10.

Li, Q., Chen, L., Li, X., Zhang, J., Zhang, X., Zheng, K., . . . Tian, X. (2016). Effect of multi-walled carbon nanotubes on mechanical, thermal and electrical properties of phenolic foam via in-situ polymerization. Composites Part A: Applied Science and Manufacturing, 214-225.

Li, X., Wang, Z., & Tsai, T. (2016). One-step in situ synthesis of a novel α-zirconium phosphate/ graphene oxide hybrid and its application in phenolic foam with enhanced mechanical strength, flame retardancy and thermal stability. RSC Advances, 74903-74912.

Ma, Z. (2022). Thermal Conductivity of Phenolic Foams. In Phenolic Based Foams Preparation, Characterization, and Applications (pp. 155-171). Springer Link.

Meyer, N., & Wollaert, G. (1984). United States of America Patent No. US4424289A.

Mougel, C., Garnier, T., Cassagnau, P., & Sintes-Zydowicz, N. (2019). Phenolic foams: A review of mechanical properties, fire resistance and new trends in phenol substitution. Polymer, 86-117.

Naseem, A., Tabasum, S., Zia, K. M., Zuber, M., Ali, M., & Noreen, A. (2016). Lignin-derivatives based polymers, blends and composites: A review. International Journal of Biological Macromolecules, 296-313.

Nasir, M., Ibrahim, M., Zakaria, N., Sipaut, C. S., Sulaiman, O., & Hashim, R. (2011). Chemical and thermal properties of lignins from oil palm biomass as a substitute for phenol in a phenol formaldehyde resin production. Carbohydrate Polymers, 112-119.

Nunes, C. S., & Kunamneni, A. (2018). Laccases—properties and applications. In Enzymes in Human and Animal Nutrition (pp. 133-161). Academic Press.

O. V. Arapova, A. V. Chistyakov, M. V. Tsodikov, I. I. Moiseev . (2020). Lignin as a Renewable Resource of Hydrocarbon Products and Energy Carriers (A Review). Petroleum Chemistry, 227-243.

Office of the Cane and Sugar Board. (2021). Situation Report of Sugarcane Planting: Production year 2020/2021. Office of the Cane and Sugar Board.

Pavia, D. L., Kriz, G. S., Lampman, G. M., & Engel, R. G. (2015). A Small Scale Approach to Organic Laboratory Techniques. Cengage Learning.

Pfungen, L. (2015). Lignin phenol formaldehyde wood adhesives.

Pilato, L. (2010). Phenolic Resins: A Century of Progress. New Jersey: Springer.

Pizzi, A., & Ibeh, C. C. (2014). Phenol-Formaldehydes. In Handbook of Thermoset Plastics (Third Edition) (pp. 13-44) . William Andrew Applied Science Publishers.

Prasara-A, J., Gweewala, S. H., Silalertruksa, T., Pongpat, P., & Sawaengsak, W. (2019) . Environmental and social life cycle assessment to enhance sustainability of sugarcane-based products in Thailand. Clean Technologies and Environmental Policy, 1447-1458.

Sarika, P. R., Nancarrow, P., Khansaheb, A., & Ibrahim, T. (2020) . Bio-Based Alternatives to Phenol and Formaldehyde for the Production of Resins. Polymers.

Sinsatitporn, T. (2019) . Study on chemical conversion behaviors of lignin from sugarcane bagasse to phenolic monomer compounds by two-step decomposition under alkaline conditions.

Srichan, T. (2020) . Optimization of Two-step Lignin Depolymerization from Sugarcane Bagasse to Phenolic Monomer Compounds under Alkaline Conditions.

Takeichi, T., & Furukawa, N. (2012). Epoxy resins and phenol-formaldehyde resins. In A. S. Abd-El-Aziz, H. Abe, Y. Abe, V. Abetz, T. W. Abraham, D. Achten, . . . A. Avgeropoulos, Polymer Science: A Comprehensive Reference (pp. 723-751).

Tang, K., Zhang, A., Ge, T., Liu, X., Tang, X., & Li, Y. (2020). Research progress on modification of phenolic resin. Materials Today Communications.

V. Karpe, A. (2015). Biodegradation of winery biomass wastes by developing a symbiotic multi-fungal consortium.

Xu, Q., Gong, R., Cui, M.-Y., Liu, C., & Li, R.-H. (2014). Preparation of high-strength microporous phenolic open-cell foams with physical foaming method. High Performance Polymers, 852-867.

Yang, W., Jiao, L., Wang, X., Wu, W., Lian, H., & Dai, H. (2020). Formaldehyde-free self-polmerization of lignin-derived monomers for synthesis of renewable phenolic resin. International Journal of Biological Macromolecules.

Youchang, J., & Srimahaprom, P. (2021). Two-step Depolymerization of Sugarcane Bagasse Lignin under Alkaline Conditions.

Yuan, H., Xing, W., Yang, H., Song, L., Hu, Y., & Yeoh, G. H. (2012). Mechanical and thermal properties of phenolic/glass fiber foam modified with phosphorus-containing polyurethane prepolymer. Polymer International, 273-279.

Yuan, J., Zhang, Y., & Wang, Z. (2015). Phenolic foams toughened with crosslinked poly (n-butyl acrylate)/silica core-shell nanocomposite particles. Journal of Applied Polymer Science, 42590.

Zhao, D., Qian, X., Gu, X., Jajja, S. A., & Yang, R. (2016). Measurement Techniques for Thermal Conductivity and Interfacial Thermal Conductance of Bulk and Thin Film Materials. JOURNAL OF ELECTRONIC PACKAGING.

APPENDIXES

APPEXDIX A
AUTOCLAVE REACTOR INSTRUCTION

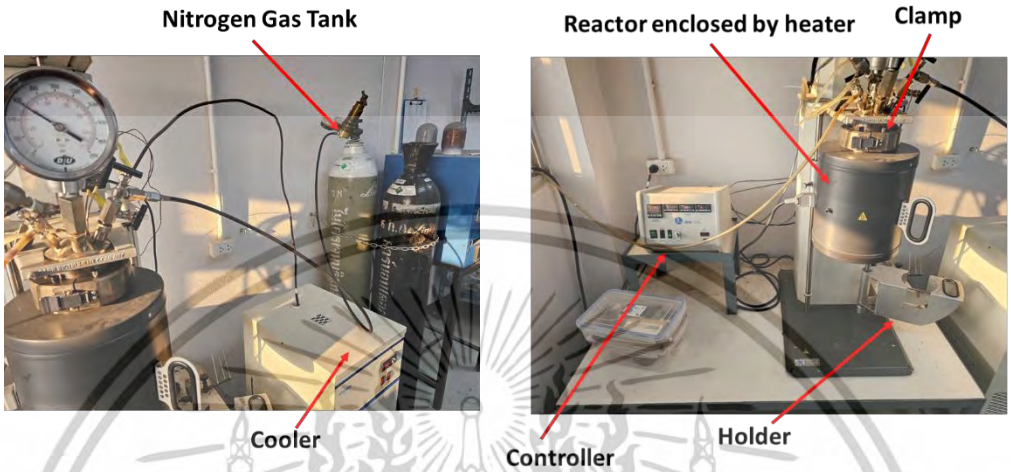

Figure A.1 Autoclave reactor instrumentation and their components.

The steps for delignification and treatment of sugarcane bagasse by using Parr reactor are following steps:

1. Wash the reactor with NaOH 4 %w/v. for 30 minutes (Mean while start the cooler machine to start lowering temperature of coolant)
2. Pour in NaOH 4%w/v (half the volume), then add Bagasse, and the rest of NaOH solution.
3. Put the reactor on the holder then move the reactor up until it is locked.
4. Put on the clamp, tighten the nuts.
5. Make sure the pressurizes tightened then lift the heater to cover the reactor then pressurize reactor with nitrogen gas, check the absolute pressure at monitor (make sure not to open any valve above reactor, except the inlet of nitrogen gas).
6. Set desired temperature and turn on the heater and stirrer at 200 rpm.
7. Wait until the temperature is set and until the reaction is completed.
8. Turn off the heater, remove the heater and cool down the reactor with an ice bath.
9. Place the holder under the reactor, remove the clamp, remove the reactor, product obtained as black liquor, wash the reactor with detergent and repeat.

APPENDIX B
DENSIMETER INSRTUCTION MANUAL

Electronic densimeter is density measurement based on the water displacement or Archimedes principle. There are following steps to measure foam density:

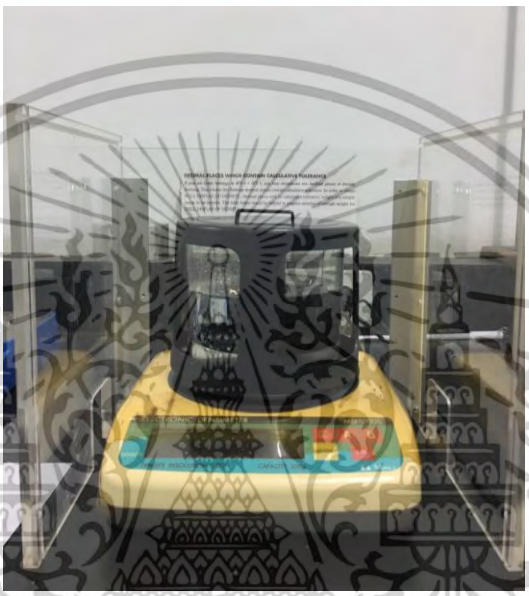

Figure B.1 Electronic densimeter MD-200S

1. Set zero to the electronic densimeter.
2. Weigh the foam on the top of electronic densimeter after then press on MEMORY to memorize the weight of solid as a dry weight.
3. Prepare methanol-water solution with ratio of 1:2 by volume.
4. Dip the foam into prepared solution in 3 to minimize the surface tension of foams that results in bubble formation during weighing in water then weigh the foam in water and press on MEMORY to memorize the weight of solid in the water.
5. Densimeter reveals density in unit of g/cm^3.
6. Discard the foam from electronic densimeter.

Caution: Loading and unloading foam samples out of the electronic densimeter requires the use of forceps to prevent water spills during foam samples handling.

APPENDIX C
RAW DATA

Table C.1 Density of PF and LPF foams obtained from electronic densimeter.

Samples	1st trial density (g/cm^3)	2nd trial density (g/cm^3)	3rd trial density (g/cm^3)	Average density of foams (g/cm^3)	Standard Deviation (g^2/cm^6)
PF	0.187	0.192	0.188	0.189	0.003
KLPF-10%	0.245	0.212	0.229	0.229	0.017
KLPF-50%	0.268	0.274	0.262	0.268	0.006
1-LPF-10%	0.245	0.239	0.221	0.235	0.012
1-LPF-50%	0.368	0.342	0.362	0.357	0.014
2-LPF-10%	0.384	0.376	0.342	0.242	0.022
2-LPF-50%	0.065	0.085	0.065	0.072	0.012

Table C.2 Temperature gradient and ambient temperature according to thermal conductivity measurement of different foams

Samples	Temperature at near heat source (T_1, ºC)	Temperature at near heat sink (T_2, ºC)	Temperature gradient (ºC)	Ambient temperature (ºC)
PF	78	46	32	30
KLPF-10%	97	42	55	30
KLPF-50%	98	41	57	30
1-LPF-10%	98	42	56	30
1-LPF-50%	106	49	57	30
2-LPF-10%	97	41	56	30
2-LPF-50%	109	50	59	30

APPENDIX D
CALCULATIONS

1. Calculation of Thermal conductivities of different lignin substitution foams

Heat source refers to stainless steel with dimensions of 10x10x0.9 cm. It is necessary to calculate actual heat transfer pass through stainless steel to the sample to calculate thermal conductivity of foam that attaches to the heat source via Fourier's law of heat conduction.

Mechanism of heat transfer from heat source to foam can be explained as heat transfer from stainless steel to foam with heat losses to ambient via radiation and natural convection to the ambient including conduction to the thermocouple wire during measuring temperature of sample and completely transfer to heat sink following the temperature gradient flows.

The steady-state model calculations of thermal conductivity of foam are divided into 3 parts: 1. heat supply to stainless steel via conduction, 2. heat loss from stainless steel to ambient via natural convection, and 3. heat conduction from stainless steel to foam.

The necessary assumptions for this experiment are 1. radiation heat transfer to ambient is negligible due to insignificantly less when compared to natural convection, 2. heat loss form conduction to thermocouples are negligible due to it is difficult to measure heat loss from conduction including thermocouples are very small then the heat loss via conduction might be insignificant. (Zhao, Qian, Gu, Jajja, & Yang, 2016)

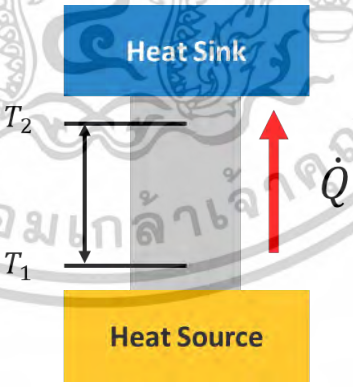

Figure D.1 Schematic of steady-state model for measuring thermal conductivity of the materials.

The example of thermal conductivity calculation of 1-LPF-50% sample is explained as below and obtained some properties from (Çengel & Ghajar, 2014)

1.1 Heat supply to stainless steel via conduction heat transfer

Heat supply to stainless steel ANSI304 was generated by conduction then Fourier's law of conduction is applied. Stainless steel has a dimension of 10x10x0.9 cm. or 0.1x0.1x0.009 m.

$$Q = \frac{kA_s}{L}(T_{1s} - T_{2s})$$

Where:

T_{1s} is the temperature of upper surface of stainless steel.

T_{2s} is the temperature of the bottom surface of stainless steel.

k is thermal conductivity of stainless steel ANSI 304 equals to 15.6 W/m·K.

A_s is a cross-sectional area of heat conduction.

L is the thickness of stainless-steel ANSI 304 which equals to 0.009 m.

$$\dot{Q} = \frac{kA_s}{L}(T_1 - T_2) = \frac{15.6\frac{W}{m \cdot K} \times 10^{-2}m^2 \times (93 - 88)K}{0.009\,m}$$

$$= 86.667\,W$$

Therefore, the heat supply to stainless steel is 86.667 W.

1.2 Heat loss from stainless-steel plate to ambient via natural convection

$$\dot{Q} = hA_s(T_s - T_\infty)$$

Where:

T_s is the temperature of upper surface of stainless steel which equals to 108°C.

T_∞ is the temperature of ambient temperature which equals to 30°C.

A_s is to surface of stainless-steel which exposed to ambient.

h is to convective heat transfer coefficient.

Firstly, determine the surface exposed to ambient.

- Stainless steel has a dimension of 10x10x0.9 cm. or 0.1x0.1x0.009 m.
- Foam sample has a dimension of 5x5x1 cm. or 0.05x0.05x0.01 m.

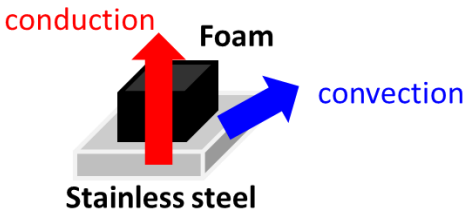

Figure D.2 Schematic heat transfer mechanism from stainless steel to foam and loss by natural convection

The area exposed to the air (A_s) = (Cross-sectional area of stainless steel) – (Area of foam occupied) + (Side areas of stainless steel)

The area exposed to the air (A_s) = (0.1 m. x 0.1 m.) – (0.05 m. x 0.05 m.) + (0.1 m. x 0.009 m.) = 0.011 m^2

Secondly, determine convective heat transfer coefficient using empirical correlation through Rayleigh number and average Nusselt number as a horizontal plate.

$$Ra_L = \frac{g\beta(T_s - T_\infty){L_c}^3}{\nu^2} Pr$$

$$Nu = 0.54{Ra_L}^{\frac{1}{4}} \ (for\ Ra\ range\ from\ 10^4 - 10^7)$$

$$Nu = 0.15{Ra_L}^{\frac{1}{4}} \ (for\ Ra\ range\ from\ 10^7 - 10^{11})$$

Where:

g	=	gravitational acceleration	(m/s^2)
β	=	Coefficient of volume expansion	
T_s	=	Temperature of surface	(°C)
T_∞	=	Temperature of air	(°C)
L_c	=	Characteristic length of geometry	(m)
ν	=	Kinematic viscosity of the fluid	(m^2/s)
p	=	Perimeter of geometry	(m)

The surface of stainless steel has a temperature of 108°C at the top.

The above properties can be found in [ref] as a film temperature.

$$T_f = \frac{T_s + T_\infty}{2} = \frac{108 + 30}{2} = 69\ °C$$

And perimeter (p) can be calculated to as result of 4x 0.1 m. = 0.4 m.

Table D.1 Properties of air at film temperature of 69°C

Properties	Value	Units	Properties	Value	Units
ρ	1.032	kg/m^3	k	0.029	W/m·K
C_p	1.010×10^3	J/kg K	Pr	0.708	-
α	2.800×10^5	m^2/s	g	9.800	m/s
μ	2.050×10^5	kg/m·s	β	0.003	K^{-1}
ν	1.980×10^5	m^2/s			

The characteristic length of the metal plate can be calculated as $L_c = \frac{A}{p}$

$$L_c = \frac{0.01\ m^2}{0.4\ m} = 0.018\ m.$$

The Rayleigh number can be calculated as

$$Ra_L = \frac{9.8\ \frac{m}{s^2} \times 0.003\ \frac{1}{K} \times (108 - 30°C)(0.018\ m)^3}{\left(1.980 \times 10^5\ \frac{m^2}{s}\right)^2} \times 0.708 = 2.650 \times 10^4$$

Then apply the empirical correlation when Ra_L is in the range of 10^4-10^7

Results in Nusselt number of

$$Nu = 0.54 \times {Ra_L}^{1/4} = 0.54 \times (2.650 \times 10^4)^{1/4} = 6.890$$

Next, calculate convective heat transfer coefficient as

$$h = \frac{Nu \times k}{L_c} = \frac{6.89 \times 0.029\ \frac{W}{m \cdot K}}{0.019\ m.} = 10.700\ \frac{W}{m^2 \cdot K}$$

Next, calculate natural convection heat transfer.

$$\dot{Q} = hA_s(T_s - T_\infty)$$

$$\dot{Q} = 10.700\ \frac{W}{m^2 \cdot K} \times 0.011 m^2 \times (108 - 30)K = 9.280\ W$$

Finally, remaining heat transfer to foam via conduction is

$$\dot{Q} = 86.667\ W - 9.280\ W = 77.400\ W$$

1.3 Heat conduction from stainless steel to foam.

The remaining heat transfer from stainless steel to foam is 77.400 W. thus, heat flux can be calculated as

$$\dot{q} = \frac{\dot{Q}}{A_{foam}} = \frac{77.400\ W}{(0.05\ m. \times 0.05\ m.)} = 3.100 \times 10^4\ \frac{W}{m^2}$$

Thermal conductivity can be determined by using Fourier's law of heat conduction.

$$k = \frac{\dot{q} \times L}{(T_1 - T_2)} = \frac{3.100 \times 10^4\ \frac{W}{m^2} \times 0.01m.}{(106 - 49)K} = 5.430\ \frac{W}{m \cdot K}$$

Finally, thermal conductivity of 1-LPF-50% is 5.430 W/m·K

Where:

T_1 is the temperature of foam near heat source (°C) = 106°C

T_2 is the temperature of foam near heat sink (°C) = 49°C

L is the thickness of the foam (m) = 1 m.

Note: Each formulation was repeated with 2 samples. Therefore, the average thermal conductivity for each formulation is needed and during the calculations, only step 3 is changed due to the variation of foams.

The results of average thermal conductivity of different foams are shown below:

Table D.2 Results of average thermal conductivity of different foams

Sample	Average thermal conductivity (W/m·K)
PF	9.135
KLPF-10%	5.630
KLPF-50%	5.480
1-LPF-10%	5.530
1-LPF-50%	5.480
2-LPF-10%	5.630
2-LPF-50%	5.295

2. Calculation of cell density with pore diameter of different lignin substitution foams

Pore diameter is measured using SEM images acquired from EVO MA10 with ImageJ. The image of 100X is used throughout all foam to be consistent. Diameter is measured two times as a cross per pore to obtained average pore diameter, each image used at least 10 pores to obtained average pore diameter.

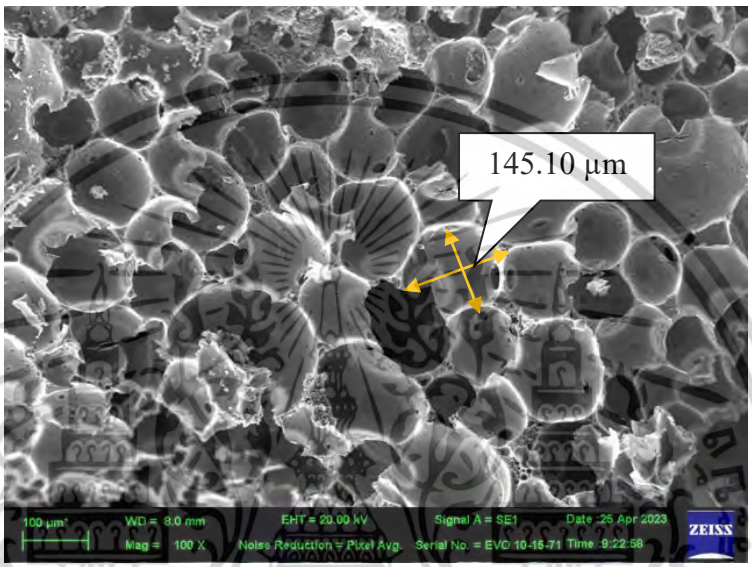

Figure D.3 Measuring average pore diameter by SEM image.

The acquired pore diameter is then averaged and noted, for this sample is 145.10 µm. The average diameter of each foam is then used in calculation of cell density as following equation:

$$N_F = \left[\frac{n}{A}\right]^{3/2}$$

Where N_F is cell density (cells/cm^3),

n is number of cells counted in area of interest (cells),

A is area of interest (cm^2).

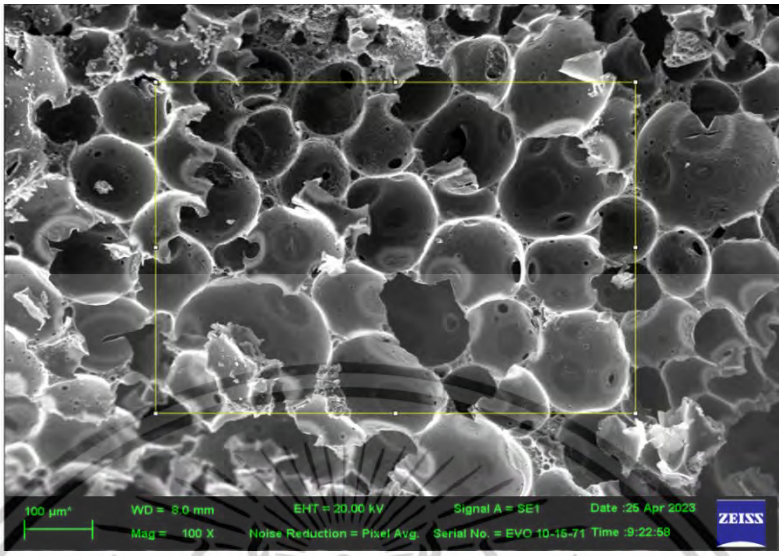

Figure D.4 Defining the interest area.

The area of interest is created and measured, 0.0036 cm^3 for this image, using ImageJ. The number of cells is counted manually, completed cell is counted as one while not-completed cell is counted as fraction according to its completeness. This image has 22.6 total cells inside the area of interest. The calculation can be done in equation as follows:

$$N_F = \left[\frac{n}{A}\right]^{3/2} = \left[\frac{22.6}{0.0036}\right]^{3/2} = 4.89 \times 10^5 cells/cm^3$$

This procedure is repeated in every SEM image of foam sample to acquire cell density of each foam. The acquired cell density is then noted and plotted as graph.

Table D.3 Results of pore diameter and cell density per volume of foams.

Sample	Average pore diameter (µm)	Area of interest (cm^3)	Cell density ($\times 10^5$ cells/cm^3)
PF	145.10	0.0036	4.89
KLPF-10%	183.55	0.0044	2.82
KLPF-50%	212.84	0.0034	2.14
1-LPF-10%	150.59	0.0039	4.36
1-LPF-50%	181.03	0.0040	1.70
2-LPF-10%	192.37	0.0055	2.08
2-LPF-50%	245.29	0.0056	0.67